POLITECNICO DI TORINO

Corso di Laurea Magistrale in Ingegneria dell'Autoveicolo

Master Degree Thesis

Predictive Maintenance for Tandem Motors

in CNC Machine

Supervisor:

Prof: Paolo Chiabert

Candidate:

Hanlin Zhang

September 2019

Predictive Maintenance for Tandem Motors in CNC Machine

Abstract

This paper outlines the application of tandem motors used as feeding device with excellent backlash performance in CNC machine and the issues related to design, manufacturing, installation and maintenance of tandem motors. Predictive maintenance based on condition monitoring is required for the industry 4.0 architecture. Monitors are used to detect the working condition of the feeding system. The data collected from monitors are regarded as the basis which provides information about the working condition. The result of this research enables manufacturers to know the best time to repair or change devices. The benefits are reducing the cost of maintenance and improving the productivity efficiency. The cost of this type of maintenance system will be affordable even for small manufacturing enterprise.

Key words: CNC machine; tandem motors; rack pinion; predictive maintenance; error detecting.

Content

List of Figures

List of Tables

1 Introduction of tandem motor and its use in CNC machines

There are several options for engineers or manufacturers designing electromechanical linear motion system in CNC machine such as linear motors, ball screws and rack-and-pinion gear drives. In this paper, the rack-and-pinion driven by motors is deeply described and analyzed (figure 1). Large-scale CNC machine needs to be equipped with high-torque servo motors to overcome friction loads, and the cost is relatively high. At the same time, because of longer stroke, the rack and pinion combination are used as the transmission mechanism, and there is a problem that the rack and pinion gap is too large.

The machine has an opposing torque anti-backlash Rack & Pinion system. There are 2 motors, 2 gearboxes, and 2 pinions driving 1 rack attached to the table. The motors drive in equal but opposite directions to create a tension torque on the rack at stand still.

In the field of industrial production, the application of servo systems is extremely extensive. Engineers are constantly researching them to get servo systems with better control performance. For position control, people pursue higher positioning accuracy of the servo mechanism; for speed control, people hope to further improve the response speed and tracking accuracy of the servo system, and at the same time have strong anti-interference ability. For heavy-duty machine tools, the servo system is required to maintain low speed under high power conditions and smoothly output high torque.

Figure 1.1 Rack Pinion anti-backlash with tandem motors

1.1 The source of gap between gears

In the transmission system of heavy machine tools, the general load side has low speed and high torque technical requirements, usually achieved by gear transmission. However, in the process of designing, manufacturing and assembling the gear, there must be a gap between the two gears, so that when the two gears mesh with the transmission, the space can generate a lubricating oil film, reduce the frictional resistance during the gear transmission, and also make the gear It won't get stuck because it is heated up. However, due to the existence of gear clearance, the performance of the servo system is seriously affected. When the gear is reversed, there is a tooth-side clearance, which will cause impact and vibration of the mechanical system, especially in the case where the accuracy and stability are high. This is unacceptable. [1]

The gear clearance is non-linear. The gap between the gear teeth caused by the nonlinear mechanical drive between the gear teeth of the gear (rack) in the mechanical transmission system is an important factor affecting the stability of the system and the poor dynamic performance. If proper measures are taken to eliminate the gear clearance, system performance

2

may be degraded or even become unstable. At the same time, the reverse of the rigid gear creates a collision with violent vibration and noise, which is especially noticeable in heavy-duty machine tools. Therefore, gear clearance compensation is an important part of high-precision precision machine tools.

1.2   Anti-backlash method

In the process of gear (rack) transmission meshing, the upper gear and the lower gear must have a tooth side clearance existing on the gear surface, otherwise there will be a jam between the gear and the gear, and two meshing forces There is a very large friction between the gears, which will greatly reduce the service life of the gears. If there is a gap between the two teeth that mesh with each other, the lubricating oil can enter the gap to form a lubricating oil film, the friction between the gears will be greatly reduced, and the gear will not die, thereby protecting the gear. However, due to the gap between the two teeth that mesh with each other, the originally ideal linear transmission becomes a nonlinear transmission.

In order to eliminate the influence of gear clearance on the accuracy of heavy machine tools, there are two main methods used at present: mechanical structure backlash method and dual motor control backlash method.

1.2.1 Mechanical structure method

The oldest method of eliminating gear gaps is the mechanical structure backlash method. The mechanical structure backlash method improves the mechanical structure of the transmission system, such as spring loaded double-gear gear clearance, and the two gears are changed to a center-adjustable mechanism. The mechanical structure backlash method can reliably avoid the influence of static error on the transmission system. The disadvantage is that the transmission mechanism is more complicated, the reliability of the transmission system is reduced, the

3

manufacturing cost is increased, and the transmission efficiency is lowered. In addition, for high-precision servo systems, the transmission system is required to be frequently and quickly commutated, and the mechanical structure backlash method cannot solve the transient error of the gap. [1]

In a conventional machine tool, only one motor is used in a certain transmission system, and the gear gap can only be compensated by various control means to reduce the influence on the gear gap. It cannot be completely eliminated.

1.2.2 Tandem motor method

The use of tandem motor drives completely eliminates the effects of backlash, so in many devices where high control accuracy is required, dual-motor drives have been widely used as a very reliable way to eliminate non-linearity of the flank clearance. In the field of high-precision CNC machine tools, radar measurement and control, and robot position control, dual motor backlash is very common.

Compared with one large servo motor, we can use two smaller servo motors which have smaller sum of torque than the larger one. The same output torque can be obtained by tandemly connecting the two small servo motors. These actuators use a single rack with two pinions and two motors, working in tandem, along with an electronic controller. They give backlash-free motion while minimizing frictional losses, making them more precise and energy efficient than ever.
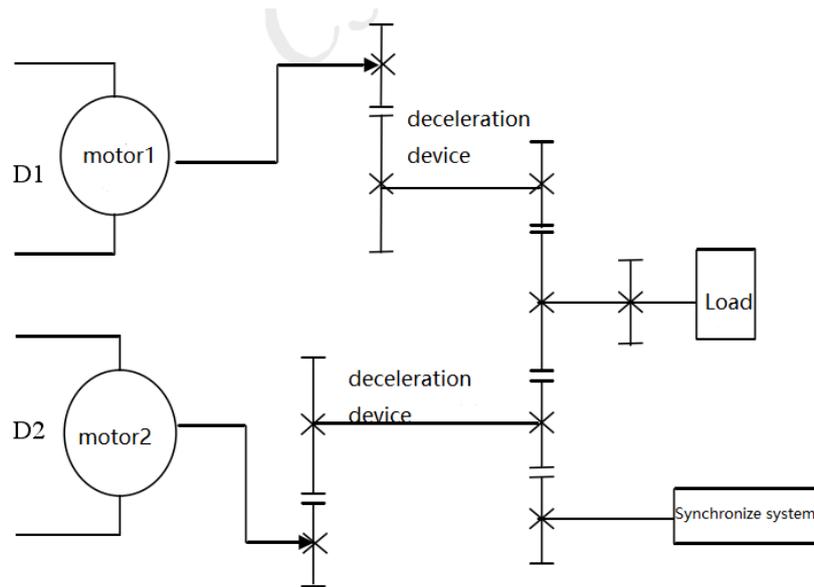
Figure 1.2 The driving elements diagram of tandem motors

Here is how it works over the four different stages of motion. [2]

Standstill. Electronic preloaded rack-and pinion drives have master and slave axes. At standstill, they generate opposing torque and the restraint, or electronic preload, is at its maximum. The master and slave engage tooth flanks facing in opposite directions to eliminate backlash or "play" in the system.

Acceleration. The controller reduces electronic preload during acceleration. The master axis initiates motion while the slave axis eases the opposing force preload. As the unit accelerates, the slave axis transitions to the opposite tooth flank and both actuators act in tandem, but still without backlash. This is important because traditional preloading does not let both axes work together. Instead, one axis always pushes against the other, creating inefficiencies.

Constant speed. During constant-speed movements, electronic preloading is disabled and both axes work together to carry the load. Inertia and workpiece resistance maintain backlash-free operation.

Deceleration. During deceleration, the slave axis again transitions to the opposite tooth flank,

5

increasing restraint to help slow the load and eliminate backlash. There is no backlash during load changes because the tooth and flanks never lose contact.

1.3   Tandem servo motors backlash principle

Compared with the parallel and series double motor drive, in the master-slave tandem motor drive, the driven motor can still follow the active motor more accurately when the active motor is subjected to external interference. Therefore, the tandem motor drive in the modern CNC machine adopts the master and slave structure. Master and slave control principle can be shown by the control block diagram.[1]
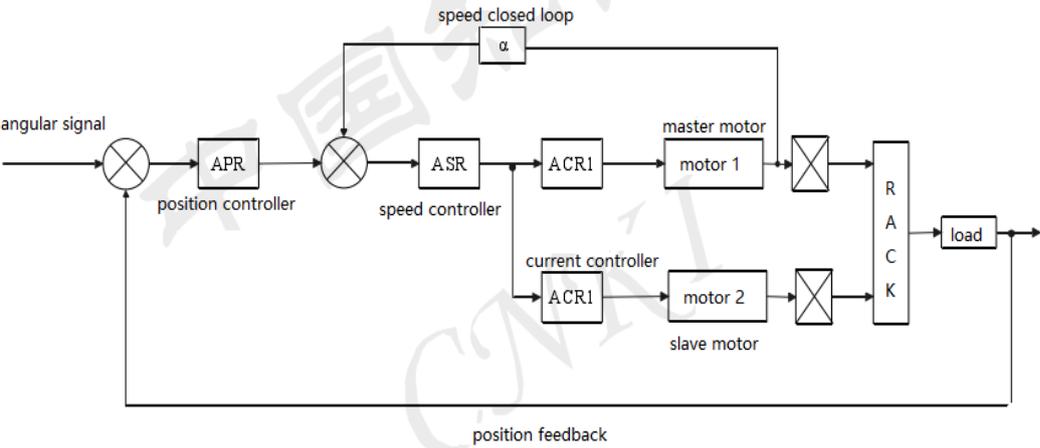
Figure 1.3 Control diagram for tandem motors

From the figure 3 we can see, in the master-slave synchronous control system, one servo motor is used as the active motor, and the other servo motor is used as the slave motor. The active motor moves at the speed and position given by the user, and the set value of the system is tracked during the motion. The motor uses the speed and position output of the active motor as its own reference value and keeps track of the active motor throughout the entire motion. The main motor has a complete speed closed loop, and the driven motor works in an open loop state, and its speed is synchronized with the main motor through gear meshing, so that the

6

synchronization accuracy of the system is greatly improved.

The dual motor backlash technology is based on a dual motor synchronous control system. The double servo motor has two sets of identical pinion gears outputting the pinion gears to drive the main shaft gears. The electric servo makes the main shaft gears always receive an offset torque during the starting and reversing process. The two output pinions are always attached to the opposite faces of the large gear during the starting and reversing directions, as shown in Figure 4, so that the large gear cannot swing back and forth in the middle of the backlash. Eliminate the gap of the drive chain and improve the positioning accuracy of the system.
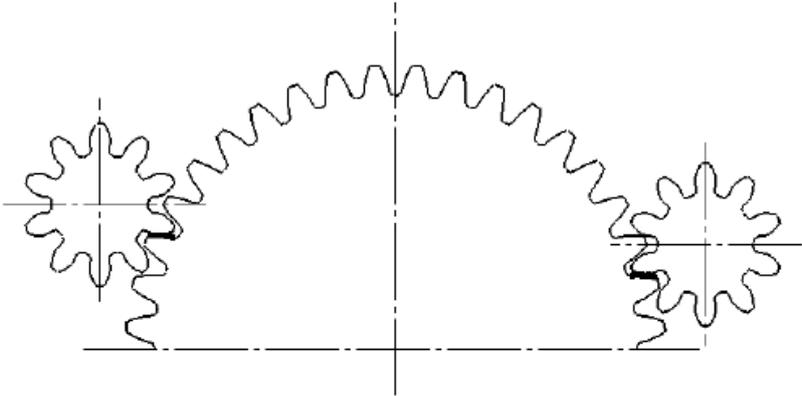
Figure 1.4 tandem gears model

2 Possible faults of tandem motors

AC asynchronous motor is the most widely used in CNC machine. The structure of this kind of motor is quite complex. Figure 5 shows the structure of rotor. Figure 6 shows the overall structure of three phase squirrel cage induction motor.
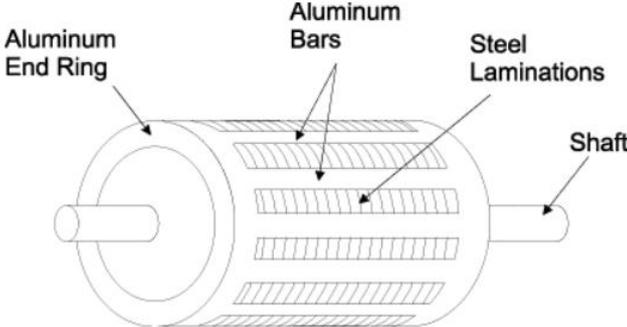
Figure 2.1 Motor rotor structure
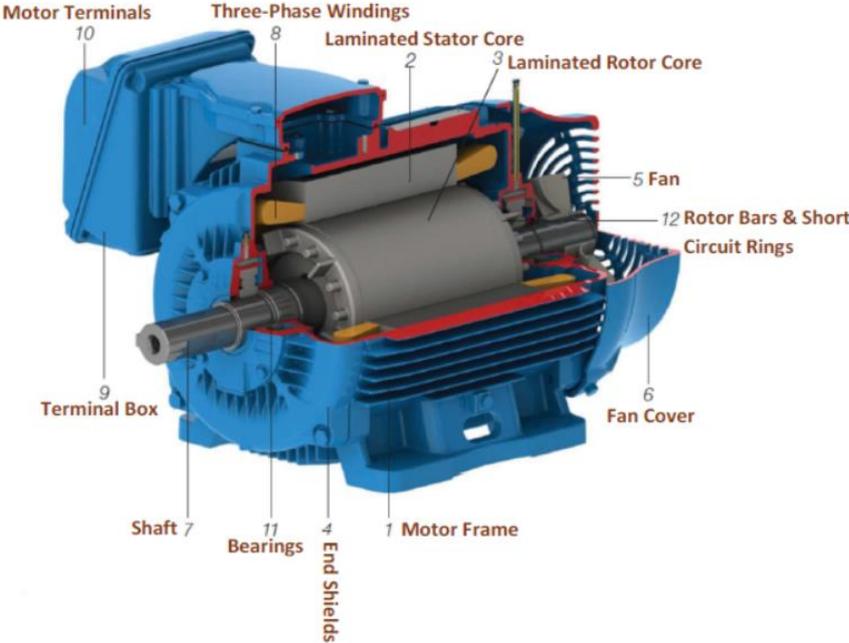
Figure 2.2 Overall structure of three phase squirrel cage induction motor.

The motor may malfunction during operation due to various reasons, and the common faults

of the motor are mainly divided into mechanical and electrical aspects.

2.1　Mechanical reasons

Rotor and stator eccentricity, vibration, bearing overheating, damage and other mechanical problems. The air gap between stator and rotor of asynchronous motor is very small, which is easy to cause the collision between stator and rotor. Usually, the eccentricity of the rotor and stator is caused by the wear of the inner hole of the end cover shaft or the deformation of the end cover and seat stop, the different positions of the base, end cover and rotor.

The vibration should be distinguished first by the motor itself, or by a poor transmission or mechanical load end, and then excluded as the case may be. Vibration caused by the motor itself is mainly due to the rotor's poor dynamic balance, poor bearing, bending of the shaft, or different ends of the end cover, base, rotor or uneven foundation. Motor, installation is not in place, fastener is loose. Vibrations create noise and create additional loads.2.2 Electrical reasons

2.2　Electrical reasons

Electrical faults include stator winding phase loss operation, stator winding end-to-end reverse connection, three-phase current unbalance, winding short-circuit and grounding, winding overheating and rotor breakage, open circuit, etc.

Phase loss operation is one of the common faults. As long as there is a phase disconnection in the three-phase power supply, the motor will run out of phase. Phase loss operation may be caused by fuse blown on the line, poor contact of the switch contacts or wire connectors.

After the three-phase motor lacks a phase power supply, if it is in the stop state, it is blocked due to the zero combined torque (cannot be started). The stall current of the motor is much larger than the normal operating current. Therefore, in this case, the power-on time is too long

or the power-on is frequently turned on several times, which will cause the motor to burn out. When the running motor lacks one phase, if the load torque is small, the operation can be maintained, only the speed is slightly decreased, and an abnormal sound is emitted; when the load is heavy, the running time is too long, and the motor winding will be burnt.

When the three-phase windings are misconnected, the three-phase current will be seriously unbalanced after the power is turned on, the speed will drop, the temperature rise will increase sharply, the vibration will increase, and the sound will change rapidly. If the protection device does not operate, it is easy to burn the motor windings. Therefore, it is necessary to discern the first and last ends of the motor outlet before it can be energized.

The failure of the three-phase current imbalance is often caused by the imbalance of the external power supply voltage of the motor; the internal cause is mainly the winding turn-to-turn short circuit or the coil turns error or wiring error when the motor is re-wound repaired.

Grounding and shorting of the winding can cause excessive current. Ground faults can be checked with a megohmmeter. The short-circuit fault can be judged by measuring the current while reducing the power supply voltage of the stator winding, or by measuring its DC resistance.

The main cause of motor overheating is that the dragged load is too heavy, and the voltage is too high or too low, which will overheat the motor. Severe overheating will cause the inside of the motor to emit an insulating charred smell. If it is not treated in time or the protection device does not operate, it is easy to burn the motor.

When the cage motor rotor cast aluminum conductor broken strip or the wound motor rotor winding is broken, the stator current is abnormal, and the high-time and low-cycle periodic changes occur, and the noise and vibration are suddenly large and small. The more severe the load, the more pronounced this phenomenon is.

In conclusion, the main faults of asynchronous motors include bearing faults, rotor bars and end ring breaks, stator winding turn-to-turn shorts, and air gap eccentricity faults. The figure 7 shows the probability of faults of different parts.
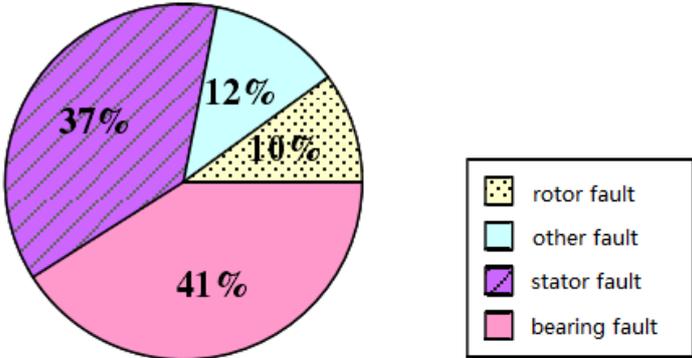
Figure 2.3 The probability of faults of different parts

Among these components, much effort is spent on rotor bar failures of induction motors. If the number of broken bars increases, reaching unacceptable operating conditions; therefore, the importance of a correct diagnosis is inevitable.

Bearing faults are over 40% of all induction machine faults, and their detection are desired to prevent damages of industrial processes.

Though rotor faults appear less significant than bearing faults in terms of quantitative manner, most of the bearing failures are caused by shaft misalignment, rotor eccentricity, and other rotor related faults.

These faults produce some symptoms such as unbalanced air-gap voltages and line currents, increased torque pulsations, decreased average torque, increased losses in efficiency, excessive heating.

3 The maintenance process

Maintenance costs, as defined by normal plant accounting procedures, are normally a major portion of the total operating costs in most plants. Industrial and process plant typically utilize two type of maintenance management: run-to-failure and preventive maintenance. Also, preventive maintenance which is new maintenance management method is applied.[3]

Because of the exorbitant nature of maintenance costs, they represent the greatest potential short-term improvement. Delays, product rejects, scheduled maintenance downtime, and traditional maintenance costs—such as labor, overtime, and repair parts—are generally the major contributors to abnormal maintenance costs within a plant.

The dominant reason for this ineffective management is the lack of factual data that quantify the actual need for repair or maintenance of plant machinery, equipment, and systems. Maintenance scheduling has been done in many instances, still is predicated on statistical trend data or on the actual failure of plant equipment.

Until recently, middle and corporate level management have ignored the impact of the maintenance operation on product quality, production costs, and more importantly on bottom-line profit. The general opinion has been ''maintenance is a necessary evil'' or ''nothing can be done to improve maintenance costs.'' Perhaps these were true statements 10 or 20 years ago. However, the developments of microprocessor or computer-based instrumentation that can be used to monitor the operating condition of plant equipment, machinery, and systems have provided the means to manage the maintenance operation. They have provided the means to reduce or eliminate unnecessary repairs, prevent catastrophic machine failures, and reduce the negative impact of the maintenance operation on the profitability of manufacturing and

production plants.

Industrial and process plants typically utilize types of maintenance management: run-to-failure and preventive maintenance. What's more, predictive maintenance which is a new maintenance method is more and more implemented in modern factories.
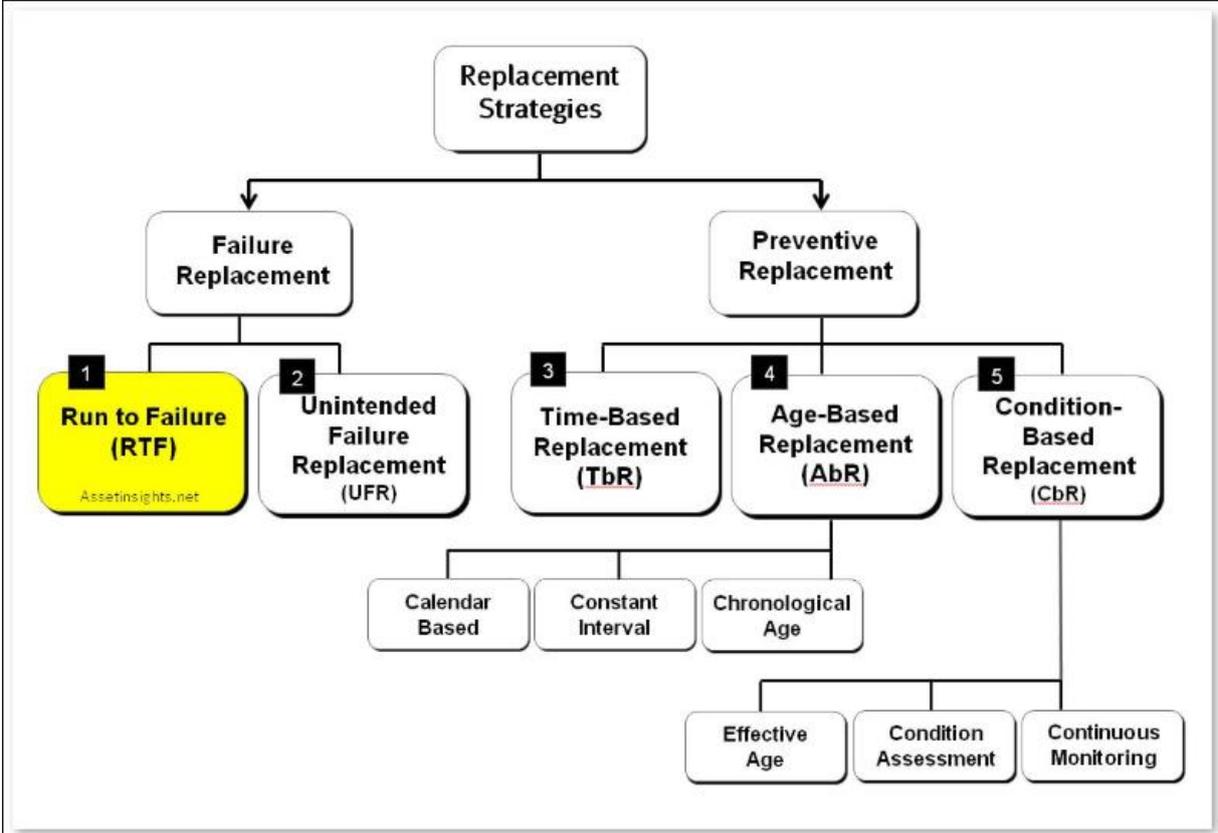
Figure 3.1 Classification of maintenance management methods

3.1   Run-to-failure management introduction

The logic of run-to-failure management is simple and straightforward. When a machine breaks, fix it. This ''if it doesn't break, don't fix it'' method of maintaining plant machinery has been a major part of plant maintenance operations since the first manufacturing plant was built, and on the surface sounds reasonable. A plant using run-to-failure management does not spend any money on maintenance until a machine or system fails to operate. Run-to-failure is a reactive

management technique that waits for machine or equipment failure before any maintenance action is taken. It is in truth a no-maintenance approach of management. It is also the most expensive method of maintenance management.

Few plants use a true run-to-failure management philosophy. In almost all instances, plants perform basic preventive tasks (i.e., lubrication, machine adjustments, and other adjustments) even in a run-to-failure environment. However, in this type of management, machines and other plant equipment are not rebuilt nor are any major repairs made until the equipment fails to operate.

The major expenses associated with this type of maintenance management are: (1) high spare parts inventory cost, (2) high overtime labor costs, (3) high machine downtime, and (4) low production availability. Since there is no attempt to anticipate maintenance requirements, a plant that uses true run-to-failure management must be able to react to all possible failures within the plant. This reactive method of management forces the maintenance department to maintain extensive spare parts inventories that include spare machines or at least all major components for all critical equipment in the plant. The alternative is to rely on equipment vendors that can provide immediate delivery of all required spare parts. Even if the latter is possible, premiums for expedited delivery substantially increase the costs of repair parts and downtime required for correcting machine failures. To minimize the impact on production created by unexpected machine failures, maintenance personnel must also be able to react immediately to all machine failures.

The net result of this reactive type of maintenance management is higher maintenance cost and lower availability of process machinery. Analysis of maintenance costs indicates that a repair performed in the reactive or run-to-failure mode will average about three times higher than the same repair made within a scheduled or preventive mode. Scheduling the repair provides the

ability to minimize the repair time and associated labor costs. It also provides the means of reducing the negative impact of expedited shipments and lost production.

3.2   Preventive maintenance management

There are many definitions of preventive maintenance, but all preventive maintenance management programs are time driven. In other words, maintenance tasks are based on elapsed time or hours of operation. Figure 1.1 illustrates an example of the statistical life of a machine-train. The mean time to failure (MTTF) or bathtub curve indicates that a new machine has a high probability of failure, because of installation problems, during the first few weeks of operation. After this initial period, the probability of failure is relatively low for an extended period of time. Following this normal machine life period, the probability of failure increases sharply with elapsed time. In preventive maintenance management, machine repairs or rebuilds are scheduled on the basis of the MTTF statistic.
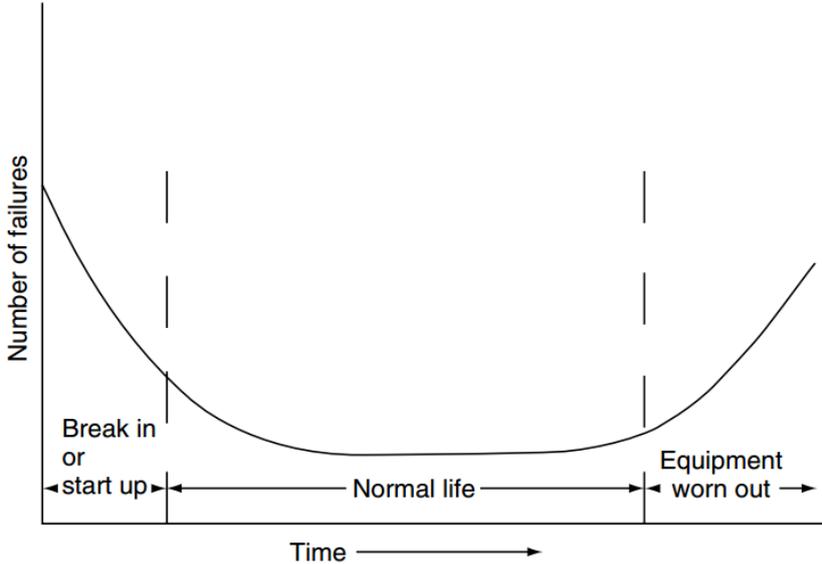
Figure 3.2 Bathtub curve

The actual implementation of preventive maintenance varies greatly. Some programs are extremely limited and consist of lubrication and minor adjustments. More comprehensive

preventive maintenance programs schedule repairs, lubrication, adjustments, and machine rebuilds for all critical machinery in the plant. The common denominator for all of these preventive maintenance programs is the scheduling guideline. All preventive maintenance management programs assume that machines will degrade within a time frame typical of its particular classification. For example, a single-stage, horizontal split-case centrifugal pump will normally run 18 months before it must be rebuilt. When preventive management techniques are used, the pump would be removed from service and rebuilt after 17 months of operation.

The problem with this approach is that the mode of operation and system or plant-specific variables directly affect the normal operating life of machinery. The mean time between failures (MTBF) will not be the same for a pump that is handling water and one that is handling abrasive slurries. The normal result of using MTBF statistics to schedule maintenance is either unnecessary repairs or catastrophic failure. In the example, the pump may not need to be rebuilt after 17 months. Therefore, the labor and material used to make the repair was wasted. The second option, use of preventive maintenance, is even more costly. If the pump fails before 17 months, we are forced to repair by using run-to-failure techniques. Analysis of maintenance costs has shown that a repair made in a reactive mode (i.e., after failure) will normally be three times greater than the same repair made on a scheduled basis.

3.3   Predictive maintenance management

Like preventive maintenance, predictive maintenance has many definitions. To some, predictive maintenance is monitoring the vibration of rotating machinery in an attempt to detect incipient problems and to prevent catastrophic failure. To others, it is monitoring the infrared image of electrical switchgears, motors, and other electrical equipment to detect developing problems.
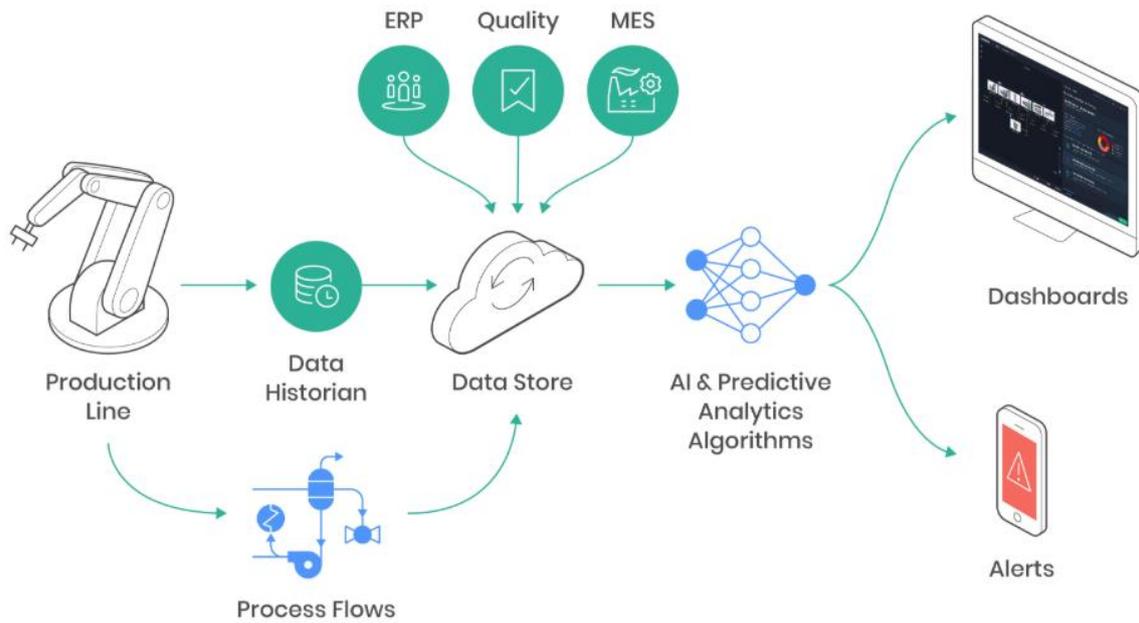
Figure 3.3 Predictive maintenance for industry 4.0

The common premise of predictive maintenance is that regular monitoring of the mechanical condition of machine-trains will ensure the maximum interval between repair and minimize the number and cost of unscheduled outages created by machine-train failures. Predictive maintenance is much more. It is the means of improving productivity, product quality, and overall effectiveness of our manufacturing and production plants. Predictive maintenance is not vibration monitoring or thermal imaging or lubricating oil analysis or any of the other nondestructive testing techniques that are being marketed as predictive maintenance tools. Predictive maintenance is a philosophy or attitude that, simply stated, uses the actual operating condition of plant equipment and systems to optimize total plant operation. A comprehensive predictive maintenance management program utilizes a combination of the most cost-effective tools—that is, vibration monitoring, thermography, tribology, etc.—to obtain the actual operating condition of critical plant systems, and based on these actual data, schedules all maintenance activities on an as-needed basis. Including predictive maintenance in a comprehensive maintenance management program will provide the ability to optimize the

17

availability of process machinery and greatly reduce the cost of maintenance. It will also provide the means to improve product quality, productivity, and profitability of our manufacturing and production plants.
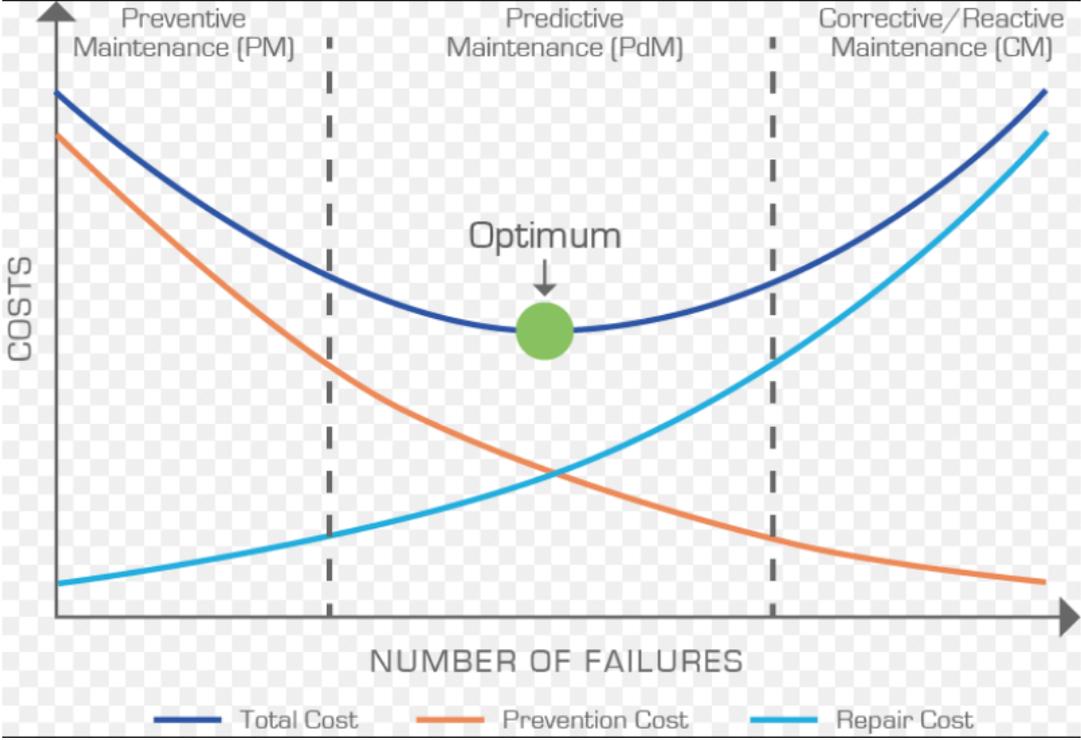
Figure 3.4 The cost of predictive maintenance

Predictive maintenance is a condition-driven preventive maintenance program. Instead of relying on industrial or in-plant average-life statistics (i.e., MTTF) to schedule maintenance activities, predictive maintenance uses direct monitoring of the mechanical condition, system efficiency, and other indicators to determine the actual MTTF or loss of efficiency for each machine-train and system in the plant. At best, traditional time-driven methods provide a guideline to normal machine-train life spans. The final decision, in preventive or run-to-failure programs, on repair or rebuild schedules must be made on the bases of intuition and the personal experience of the maintenance manager. The addition of a comprehensive predictive maintenance program can and will provide factual data on the actual mechanical condition of

each machine-train and operating efficiency of each process system. These data provide the maintenance manager with actual data for scheduling maintenance activities.

A predictive maintenance program can minimize unscheduled breakdowns of all mechanical equipment in the plant and ensure that repaired equipment is in acceptable mechanical condition. The program can also identify machine-train problems before they become serious. Most mechanical problems can be minimized if they are detected and repaired early. Normal mechanical failure modes degrade at a speed directly proportional to their severity. If the problem is detected early, major repairs, in most instances, can be prevented. Simple vibration analysis is predicated on two basic facts: all common failure modes have distinct vibration frequency components that can be isolated and identified, and the amplitude of each distinct vibration component will remain constant unless there is a change in the operating dynamics of the machine-train.

Predictive maintenance that utilizes process efficiency, heat loss, or other nondestructive techniques can quantify the operating efficiency of non-mechanical plant equipment or systems. These techniques used in conjunction with vibration analysis can provide the maintenance manager or plant engineer with factual information that will enable him to achieve optimum reliability and availability from the plant.

There are five nondestructive techniques normally used for predictive maintenance management: (1) vibration monitoring, (2) process parameter monitoring, (3) thermography, (4) tribology, and (5) visual inspection. Each technique has a unique data set that will assist the maintenance manager in determining the actual need for maintenance. Most comprehensive predictive maintenance programs will use vibration analysis as the primary tool. Since the majority of normal plant equipment is mechanical, vibration monitoring will provide the best tool for routine monitoring and identification of incipient problems.

4 Possible methods to detect the errors of tandem motors

High voltage motors are widely used in petrochemical industry. In many important applications, it is important to reduce the number of failures to an absolute minimum. For example, electric motors are usually started directly online. This results in large starting current and torque pulsation; It is assumed that these conditions contribute to end winding, rotor and bearing failures. Voltage imbalance in the power supply can also lead to winding failure. In addition, some electricity may be damp. [4]

Equipment diagnosis technology adopts advanced test and analysis instruments to carry out real-time monitoring and status identification of operating equipment, detect whether it is running normally, and provide fault warning. Like other equipment, the motor will be subjected to mechanical stress, thermal stress and electromagnetic stress during operation, which will generate various information reflecting the operating state of the system. These changes directly or indirectly reflect the running state of the motor. In the normal state and abnormal state, the information change rules are different, motor diagnosis technology USES the characteristic information to judge whether the motor running state is normal or not. Motor fault diagnosis process and other equipment the same, mainly composed of three parts.

(1) Abnormal inspection. The motor running state is analyzed by a simple detecting device or instrument to realize the preliminary identification of the motor state. If the test result is normal, no further operations are required; if the result is abnormal, a more in-depth troubleshooting is required.

(2) Fault status and location diagnosis. After the motor is detected abnormal, the sensor is used to collect the motor's running state information, conduct data analysis and signal processing, and extract the characteristic signals directly related to the fault, so as to determine the fault state and position.

 (3) Fault type and cause analysis. Identify the motor state and determine the fault type and cause according to the mechanism and characteristics of each fault mode.

Among them, the detection of motor fault state is the core part of the diagnosis, usually including information acquisition, signal acquisition, signal processing, analysis and diagnosis. Figure below shows the flow chart of the motor equipment diagnostic process.
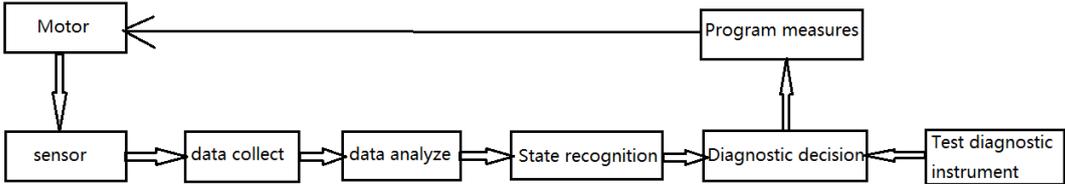
Figure 4.1 Motor equipment diagnostic process.

Several types of sensors are available for fault detection. The main groups are mechanical (vibration, impulse, acoustics, velocity fluctuations) and electromechanical (current, air-gap torque, instantaneous stator power, magnetic field, surge, partial discharge). Certain temperature, oil particle, gas analysis and performance and visual methods are also used. Because faults and their causes are so diverse, reliable fault detection must be based on a combination of methods. Condition monitoring means continuous or periodical observing of the motor condition. Condition monitoring is applied as a diagnostic tool, both for fault detection and as a basis for maintenance planning. Common methods for condition monitoring

21

follow:

4.1   Performance Monitoring

Performance monitoring involves on-line measurement of motor parameters such as power supply voltage and current, input and output power, mechanical stress in coupling, etc.

4.2   Vibration Monitoring

Vibration monitoring USES vibration sensors such as piezoresistive accelerometers with a linear spectrum. An imbalance of magnetic, mechanical, and/or aerodynamic forces causes vibrations. The measured parameters are displacement, velocity and acceleration. Vibrations are measured directionally, radial or axial, and transducers are usually placed on bearings to detect mechanical faults. By placing sensors on the stator, however, problems such as non-air gaps, stator or rotor faults, asymmetric power supplies, and unbalanced loads on the motor can also be detected. Measurements or records based on the entire spectrum or some key frequency component are compared with measurements recorded when the machine is new (or under known conditions). The sensitivity of this method is quite high.[5]

4.3   Shock Pulse Monitoring (SPM)

The SPM involves applying piezoelectric transducers to bearings to detect shock waves caused by functional components affecting defective parts, such as inner/outer rings or cracks in rolling elements in the bearing. Cracks in the rotating seat generate impulse pulses whose intensity varies with the load on the rolling element. On the other hand, cracks in the stationary seat ring generate pulses whose intensity is independent of bearing load.

4.4   Acoustic Emission Monitoring

The method utilizes ultrasonic and audible frequencies. Contact between cracked and

uncracked rolling elements produces a shock wave that travels through the machine at the speed of sound.

4.5   Speed Fluctuations Monitoring

The method detects defects by measuring the fluctuation of motor rotation period. This method is especially useful for detecting rotor faults, vibration, air gap eccentricity, rotor asymmetry, damaged bearing/coupling and misalignment. However, since in most cases the motor is subjected to a variable load torque, the measuring instrument must be able to distinguish between changes in velocity due to load changes and fluctuations indicating rotor faults.

4.6   Current Monitoring

This method analyzes the power supply current of the motor because it indicates the condition of the motor to a large extent. Current analysis may reveal damaged rotor bars and other mechanical problems.

4.7   Air-Gap Torque Monitoring

Air gap torque monitoring can detect motor faults during startup and operation. The method can detect cracked rotor bar and short-circuit stator coil. The shape of the airgap torque curve can be used to distinguish the imbalance caused by rotor bar rupture from the imbalance caused by stator winding fault.

4.8   Magnetic Field Monitoring

Under normal conditions, the magnetic field in the air gap varies sinusoidal in space and time. Some stator and rotor faults cause sinusoidal variations in deviation. Therefore, rotor faults can be detected by a search coil fixed to the stator. IN addition, a failure-related change in the air-gap flux density caused by the rotor or stator will generate axial flux that can be detected by

measuring coils around the axis or by other sensing devices, such as hall probes. By monitoring the axial flux, it is generally possible to identify various asymmetric and fault conditions, such as rotor bar damage, stator winding short-circuit between turns, phase loss, eccentricity, etc.

4.9   Visual Monitoring

Visual surveillance requires real-time inspection by naked eye or closed-circuit television, or delayed inspection by film or video to determine deviations.

The following test methods should also be mentioned.

•*Surge testing* is a well-known method for diagnosing winding faults. Surge testing usually reveals insulation faults between windings, coils and coil groups.

• *Measuring of partial discharges* may provide a measure of the condition of a motor's insulation properties.

• *Oil particle analysis is presently* is not much used for motors, but it may be useful for some motors that use cyclic lubrication systems. This analysis is designed to identify metals, fibers or dust particles in the oil.

• *Gas analysis* has shown to be a useful method for large motors. Analysis of possible carbon monoxide gases in cooling air is usually caused by deterioration of electrical insulation. In this way, overheating of the winding can be detected.

4.10   Infrared thermography

Infrared thermal imaging is a public technology in the field of electrical engineering. For decades, it has been a very useful tool for regularly checking electrical installations and distribution lines. For example, infrared cameras have been used to detect defects in electrical

switchboards, power cables, electrical switchgear, or power meters. In the field of motor state monitoring, infrared thermal imaging has become the first choice for detecting unexpected faults of power transformers in substations, power plants and industrial facilities. In fact, an intelligent fault diagnosis method based on image processing has been proposed. Literature analysis based on infrared image of transformer. Excellent review work, in-depth use of infrared thermal imaging technology for electrical equipment inspection and other applications can be found. [6]

Figure 4.2 Infrared thermography camera

The application of infrared thermal imaging in motor state monitoring is more limited. In dc motors, infrared thermal imaging is a useful tool for detecting possible defects in commutator and brush systems that are weak links from a maintenance point of view. In addition, some work has been done to develop techniques for detecting faults in the excitation windings of such machines. In wound rotor induction motors and synchronous motors and generators, infrared data analysis can provide very interesting information about the state of the sliding ring brush system, indicating possible asymmetric or defective contacts. For most of these machines, infrared thermal imaging is typically used for standard off-line testing as a core loop test (or

loop test) to detect insulation failures between the core layers. In general, however, the use of this technology is limited to detecting defective connections, and infrared technology is often used outside the machine itself to detect problems such as misaligned shafts. Some work has even expanded the use of infrared thermal imaging to analyze the effects of possible motor failures on the motor chain, while others have suggested applying this technique to the periodic maintenance and inspection of motors. Despite the previous facts, infrared thermal imaging seems to be a very interesting option, considering that most motor failures usually lead to temperature increases (generally or in specific areas) that can be detected by infrared data analysis. On the other hand, although infrared cameras were too expensive only a few years ago, there are now infrared data acquisition devices with very affordable prices and advanced features (such as high image resolution or the possibility of acquiring images during transient mechanisms).These facts give the technology great potential because it could easily be an excellent source of information for monitoring the state of rotating motors.

Application of Infrared Thermography to Failure Detection in Industrial Induction Motors: Case Stories

Table 4-1 Thermographic survey suggested action based on ΔT in electrical equipment.

Temperature difference (ΔT) based on comparisons between similar components under similar loading.	Temperature difference (ΔT) based upon comparisons between component and ambient air temperatures.	Recommended Action
1–3 °C	1–10 °C	Possible deficiency; warrants investigation
4–15 °C	11–20 °C	Indicates probable deficiency; repair as time permits
–	21–40 °C	Monitor until corrective measures can be accomplished
> 15 °C	> 40 °C	Major discrepancy; repair immediately

Table 4-2 General alarm thresholds adopted for different diagnosed components.

Element	Temperature Threshold
Motor frame	> 70 °C
Gears (reducers, multipliers, etc.)	> 80 °C
Bearings	> 70 °C
Couplings	> 80 °C
Belt transmissions	> 90 °C

As a comprehensive research field involving extensive knowledge, motor fault diagnosis technology has the characteristics of universality and openness. In recent decades, with the continuous development of computer technology, virtual instrument technology, frequency control technology and other fields, cross integration further promotes the maturity and

improvement of fault diagnosis technology and methods. The researchers divided the motor fault diagnosis methods into three aspects, including: **(1) Method based on analytical model.** The analytical methods based on the analytical model have achieved important theoretical results, including parameter estimation, state estimation and equivalent space method. However, this method requires a more accurate representation of the motor model, and there are many practical problems that cannot be solved by complex nonlinear systems.

(2) Signal processing-based method. The signal processing method avoids the difficulty of establishing the mathematical model of the diagnosis object to some extent. On the basis of in-depth analysis of fault mechanism, symbol and law, the electric quantity, vibration quantity and local discharge quantity of the motor are directly adopted as feature monitoring, signal processing and analysis, which has strong adaptability and is theoretically applicable to linear and nonlinear systems.

(3) Knowledge-based approach. With the continuous development of computational science and artificial intelligence methods, knowledge-based methods such as fuzzy logic, fault tree, expert system and neural network have also been studied and applied in the field of motor diagnosis. This method has a significant impact on the diagnosis of complex systems and processes. At present, the universality of the algorithm and further research and improvement of the main problems.5 The proposal solution and implementation method for tandem motor working condition monitoring

5 Proposal method for tandem motor fault diagnose

5.1   MCSA method overview

"Motor current signature analysis (MCSA)" are chosen due to its less expensive sensors or specialized tools compared with other faults diagnostics methods.

Motor current characteristic analysis is a non-invasive detection technology, which is one of the most effective methods for AC motor condition monitoring and fault diagnosis. A large number of literatures are based on MCSA theory to analyze and study the faults of motor rotor broken strips, stator. The current signal has become one of the main parameters for various types of motor fault diagnosis. Because the current sensor is easy to install, the stator current signal is easy to obtain, and the current signal is minimally affected by the environment and other parameters relative to other parameters. It is not necessary to evaluate other characteristic parameters of the motor during diagnosis. Although MCSA is the most effective method in the field of motor fault diagnosis, it also has certain limitations and shortcomings. First, in order to ensure the reliability of the diagnosis results, the accuracy of the slip rate is highly demanded. Secondly, the ambiguous current harmonic component has an unknown effect on the analysis and diagnosis based on the current signal. In response to the above shortcomings, many scholars have combined MCSA with advanced signal processing technology to extract effective motor fault information through current signal spectrum analysis. This method has been successfully applied to large-scale induction motor rotor fault diagnosis in industrial fields. [7]

5.1.1 MCSA common processing methods

When a device is running, it usually contains a lot of information that has nothing to do with fault characteristics. It is necessary to use modern signal processing and analysis technology to extract the characteristic parameters reflecting the state of equipment from the field data. In fault diagnosis, feature extraction is the bottleneck of its research, and signal processing technology is the core of fault feature extraction. Fault feature extraction, through the analysis and processing of the original signal, fault feature extraction, for more effective fault pattern recognition and diagnosis conditions. At present, the analysis of motor stator current signal is generally based on the fast Fourier transform (FFT), which converts the time-domain signal into the frequency domain signal, so that the characteristic signal which is difficult to observe in the time domain can be clearly seen in the frequency domain. Come out. However, the components of the Fourier transform process make the signal smooth and do not handle non-stationary signals. At the same time, Fourier transform will cause spectrum leakage, fence effect and other phenomena, affecting the accuracy of fault signal analysis. In view of the above deficiencies, domestic and foreign scholars have explored many signal processing methods to extract fault characteristic signals in recent years. More MCSA signal processing methods include: (1) Short time Fourier transform method

Short Time Fourier Transformation (STFT) is the earliest method to find and process non-stationary signals. It divides the time domain signal into many small-time segments and uses Fourier transform (FT) pairs. The analysis and processing of the data of each time interval overcomes the defect that the Fourier transform does not have the time-frequency local analysis ability to some extent. However, the windowing function of the STFT is fixed, which will result in fixed time-frequency resolution of data processing. [8]

(2) Bispectrality analysis method

Spectrum is also called third-order spectrum. Sometimes the analysis of second-order power spectrum is difficult to meet the diagnosis and recognition of mechanical faults, while high-order spectrum can well maintain the amplitude and phase characteristics of signals, suppress noise interference, and characterize Nonlinear features or identification of nonlinear systems. A large number of research results show that the spectrum analysis of stator current can provide an effective basis for motor condition monitoring and diagnosis.

(3) Park vector transformation and extended Park vector transformation

The Park vector transformation method processes the motor current signal, which can visually reflect the fault feature state image in the graph, but its recognition effect on the early fault state is not very satisfactory. Based on this, an extended Park vector transformation method is proposed, which is to analyze the current vector mode of Park transform, further weaken the interference of the fundamental frequency component, and express the fault characteristics on the frequency domain spectrum.

(4) Rotational coordinate transformation

The three-phase current signal is converted into two equivalent coordinate reference systems based on the coordinate transformation, and the motor fault is detected by the spectral characteristic of the magnetic-torque current signal, and the stator three-phase current fundamental component is converted into a two-phase DC component to highlight the fault. The characteristic frequency of the sideband component can effectively suppress the influence of power frequency interference on the characteristic signal. However, this method needs to know the operating frequency of the grid, so the expected effect cannot be achieved when the grid quality is poor.

(5) Power frequency elimination method

The power frequency elimination method refers to the pre-processing performed before the spectrum analysis of the collected current signal, thereby highlighting the fault characteristic signal, such as adaptive filtering, Hilbert transform, etc., but the existing filtering means are usually difficult to The power frequency component is completely offset, so the method is less effective for fault feature recognition.

5.1.2 Principle of rotor broken bar fault diagnosis based on stator current characteristics

When the ideal asynchronous motor is running in normal state, its stator winding current frequency f_1 is consistent with the grid frequency f. Under the structure of the three-phase symmetrical winding, the three-phase symmetrical current in the stator loop will generate a rotating magnetic field with frequency f_1=f. According to the principle of electromagnetic induction, the rotor circuit induces a positive sequence rotating magnetic field of frequency f_2=sf_1, where s is the motor slip rate. If there is a broken bar or other fault in the rotor winding of the motor, a rotating magnetic field with a frequency of sf_1 will be generated. In addition to the original positive-sequence magnetic field, a negative-sequence magnetic field of reverse rotation is added. These two induced magnetic fields will generate voltage and current signals with a characteristic frequency of (1±2s) f_1 in the stator winding, and appear as (1± 2s) f_1 side frequency components in the stator current spectrum.

5.1.2.1 Low frequency harmonic characteristics analysis

$$m_1 = K_1 N_1 I_1 \sin(\omega t - p\theta) \tag{5.1}$$

Where K_1 is a constant related to the pole pair and winding coefficient, N_1 is the number of turns per phase of the stator winding, I_1 is the stator current, and θ is the initial phase angle expressed by the mechanical angle.

32

Making the phase angle of the rotor $\varphi = \theta - \omega_r t$, substituting to equation (5.1), then for two pole motor (p=1), we have:

$$m_1 = K_1 N_1 I_1 \sin[(\omega - \omega_r)t - \varphi] \tag{5.2}$$

It can be seen from equation (5.2) that m_1 moves relative to the rotor at a differential angular velocity of $(\omega - \omega_r)$, and the rotor winding generates an induced electromotive force under the action of the rotating magnetic field of the stator, and establishes the rotor magnetomotive force for balancing the stator magnetomotive force. The fundamental expression of the rotor magnetomotive force m is:

$$m_1 = K_2 N_2 I_2 \sin[(\omega - \omega_r)t - \varphi] \tag{5.3}$$

Among them, K_2 is a constant related to the pole logarithm and winding coefficient, N_2 is the number of turns per phase of the rotor winding, and I_2 is the rotor winding current. When the rotor winding fails, if there is a broken strip, the magnetomotive force of the rotor current will be modulated by $\sin(2\varphi)$, At this time, the fundamental magnetomotive force of the rotor winding becomes:

$$\begin{aligned} m_2 &= K_2 N_2 I_2 \sin[(\omega-\omega_r)t-\phi]\sin 2\phi \\ &= \frac{K_2 N_2 I_2}{2}\{\cos[(\omega-\omega_r)t-3\phi]-\cos[(\omega-\omega_r)t-\phi]\} \end{aligned} \tag{5.4}$$

Because the rotor magnetomotive force and the stator magnetomotive force are balanced, $m_1=m_2$, substituting $\varphi = \theta - \omega_r t$, we can have:

$$m_1 = \frac{K_2 N_2 I_2}{2}\{\cos[(\omega-2\omega_r)t-3\theta]-\cos[(\omega-2\omega_r)t+\theta]\} \tag{5.5}$$

For two-pole motors, the slip ratio is $s = \frac{\omega-\omega_r}{\omega}$, as:

$$\omega_r = (1 - s)\omega \tag{5.6}$$

Substituting equation (5.6) into equation (5.5) gives the expression of the magnetomotive fundamental wave of the stator winding:

$$m_1 = \frac{K_2 N_2 I_2}{2} \{\cos[(3-2s)\omega t - 3\theta] - \cos[(1-2s)\omega t - \theta]\}$$

(5.7)

It can be seen from (5.7) that the first term of the magnetomotive force expression of the stator winding exists $3\omega t$ and 3ϑ. During the operation of the three-phase stator winding, this component will induce the zero-sequence electromotive force, which will not affect the power supply current. In the second term, there is a component that is $2s\omega$ lower than the grid frequency. This component will produce a three-phase current component in the stator winding that is $2s\omega$ lower than the source current angular frequency. Since the slip rate is very small, the current component is very close to the grid frequency. Under its modulation, the stator current will periodically fluctuate, causing the motor torque to pulsate, so that the speed of the asynchronous motor rotor is also frequency fluctuations.

5.1.2.2 High frequency harmonic characteristics analysis

When a current component with a characteristic frequency of $(1-2s)f_1$ appears in the stator current, under its action, the rotor speed will fluctuate, causing a change in the air gap flux, which will affect the induced electromotive force. The generation of the high-order harmonic component $(1+2s)f_1$ of the characteristic frequency signal is generated. The mechanism is expressed as follows:

It is assumed that the fundamental current of the stator winding and the current signal when the rotor is faulty can be expressed as:

$$i_1 = I_1 \cos(\omega t - \alpha_I)$$

(5.8)

$$i_{(1-2s)f_1} = I_{(1-2s)f_1} \cos[(1-2s)\omega t - \alpha_{I(1-2s)f_1}]$$

(5.9)

34

Where I_1 is the amplitude of the fundamental wave current of the stator, α_I is the initial phase of the fundamental current, and $I_{(1-2s)f1}$, which is the amplitude of the corresponding current of the rotor fault characteristic $(1-2s)f_1$, $\alpha_{I(1-2s)f1}$ is the initial phase of the corresponding current when the rotor fault characteristic frequency is $(1-2s)f_1$.

(1) When the motor is normal

The fundamental expression of the air gap flux is:

$$\varphi(t) = \varphi \cos(\omega t - \alpha_\varphi) \tag{5.10}$$

Where φ is the amplitude of the fundamental magnetic flux and α_φ is the initial phase of the fundamental magnetic flux.

The fundamental current interacts with the fundamental flux and the resulting torque expression is as follows:

$$T_1 = 3p\phi I_1 \sin(\alpha_\phi - \alpha_I) = T_{1m}\sin\alpha_{\phi I} \tag{5.11}$$

Among them, T_1. For the torque amplitude, $\alpha_{\phi I}$ is the angular displacement between the fundamental current and the flux.

In the formula (5.11), the torque amplitude and the angular displacement difference $\alpha_{\phi I}$ are both constant values. It can be seen that the torque generated by the stator current is a constant value under normal motor condition, that is, the motor always performs energy conversion under steady state.

(2) When the rotor fails

When the rotor breaks the fault, in addition to the fundamental current and the magnetic flux to generate torque, the current component with a characteristic frequency of $(1-2s)f_1$ will also interact with the fundamental magnetic flux to generate additional torque, which is expressed.

The formula is:

$$\Delta T_{(1-2s)f_1}(t) = 3p\phi I_{(1-2s)f_1} \sin[2s\omega t - (\alpha_\phi - \alpha_{(1-2s)f_1})]$$
$$= \Delta T_{(1-2s)f_m} \sin[2s\omega t - (\alpha_\phi - \alpha_{(1-2s)f_1})] \qquad (5.12)$$

Among them, $\Delta T_{(1-2s)fm}$ is the torque amplitude when the fault frequency is $(1-2s)f_1$.

It can be seen from the formula (5.12) that after the motor rotor fails, the torque that changes periodically according to the grid frequency twice will occur, which will cause the speed change. That is, the additional torque can be expressed by the following equation of motion:

$$\Delta T_{(1-2s)f_1}(t) = J\frac{d\Delta\omega_r(t)}{dt} \qquad (5.13)$$

Where $\Delta\omega_r(t)$ is the rotational angular velocity of the rotor and J is the rotational inertia of the system.

For the integral of equation (5.13), the wave equation of the rotor speed can be obtained:

$$\Delta\omega_r(t) = \frac{1}{J}\int \Delta T_{(1-2s)f_1}(t)$$
$$= -\frac{3p\phi I_{(1-2s)f_1}}{2sJ\omega} \cos[2s\omega t - (\alpha_\phi - \alpha_{(1-2s)f_1})]$$
$$= -\frac{\Delta T_{(1-2s)f_m}}{2sJ\omega} \cos[2s\omega t - (\alpha_\phi - \alpha_{(1-2s)f_1})]$$
$$= -\Delta\omega_{rm} \cos[2s\omega t - (\alpha_\phi - \alpha_{(1-2s)f_1})] \qquad (5.14)$$

Among them, $\Delta\omega_{rm}$ is the amplitude of the speed fluctuation.

It can be seen from equation (5.14) that the rotor's speed change frequency is consistent with the rotor's additional torque frequency under the influence of the torque action. The amplitude of the speed fluctuation is inversely proportional to the moment of inertia of the system. When the moment of inertia of the system tends to infinity, the rotor speed can be considered to be

constant, that is, the rotor breakage fault has little effect on the current signal. However, it is impossible to produce a device that satisfies this condition in practical applications, and therefore, it is usually necessary to consider the influence of the speed change on the system.

Fluctuations in rotor speed cause changes in the mechanical angle during stator operation:

$$\Delta\theta=\int\Delta\omega_r(t)\mathrm{d}t$$
$$=\int-\frac{\Delta T_{(1-2s)f_m}}{2sJ\omega}\cos[2s\omega t-(\alpha_\phi-\alpha_{(1-2s)f_1})]$$
$$=\frac{\Delta T_{(1-2s)f_m}}{4s^2J\omega^2}\sin[2s\omega t-(\alpha_\phi-\alpha_{(1-2s)f_1})] \tag{5.15}$$

From equation (5.15), the mechanical angle is also periodically changed by 2s times the grid frequency, and the change is modulated by the phase angle of the fundamental magnetic flux of the air gap, that is, the equation (5.10) becomes:

$$\phi(t)=\phi\cos(\omega t-\alpha_\phi-p\Delta\theta)$$
$$=\phi\cos\{\omega t-\alpha_\phi-\frac{p\Delta T_{(1-2s)f_m}}{4s^2J\omega^2}\sin[2s\omega t-(\alpha_\phi-\alpha_{(1-2s)f_1})]\}$$
$$=\phi\cos(\omega t-\alpha_\phi)\cos\{\frac{p\Delta T_{(1-2s)f_m}}{4s^2J\omega^2}\sin[2s\omega t-(\alpha_\phi-\alpha_{(1-2s)f_1})]\}$$
$$+\phi\sin(\omega t-\alpha_\phi)\sin\{\frac{p\Delta T_{(1-2s)f_m}}{4s^2J\omega^2}\sin[2s\omega t-(\alpha_\phi-\alpha_{(1-2s)f_1})]\} \tag{5.16}$$

In the equation (5.16), let $\eta = \frac{p\Delta T_{(1-2s)fm}}{4s^2J\omega^2}\sin[2s\omega t-(\alpha_\varphi-\alpha_{(1-2s)f1})]$ and the function terms $\cos\eta$ and $\sin\eta$ will be expanded into a Taylor series at zero. Considering that the amount of torsional change caused by the fault state is small, the Taylor expansion of the sine and cosine function in equation (5.16) ignores the higher order component, taking only the first term and becomes:

$$\phi(t) = \phi\cos(\omega t - \alpha_\phi) + \phi\frac{p\Delta T_{(1-2s)f_m}}{4s^2 J\omega^2}\sin[2s\omega t - (\alpha_\phi - \alpha_{(1-2s)f_1})]\sin(\omega t - \alpha_\phi)$$

$$= \phi\frac{p\Delta T_{(1-2s)f_m}}{8s^2 J\omega^2}\{\cos[(1-2s)\omega t - \alpha_{(1-2s)f_1}] - \cos[(1+2s)\omega t - (2\alpha_\phi - \alpha_{(1-2s)f_1})]\}$$

$$+ \phi\cos(\omega t - \alpha_\phi) \tag{5.17}$$

It can be seen from the equation (5.17) that the air gap flux at this time contains an additional flux component of $(1\pm2s)f_1$ in addition to the fundamental flux component. This flux component will be generated in the stator winding. Additional induced electromotive force and additional current. The induced electromotive force can be expressed as follows:

$$e_{(1-2s)f_1} = -m\phi\frac{p\Delta T_{(1-2s)f_m}}{8s^2 J\omega^2}(1-2s)\omega\sin[(1-2s)\omega t - \alpha_{(1-2s)f_1}]\} \tag{5.18}$$

$$e_{(1+2s)f_1} = m\phi\frac{p\Delta T_{(1-2s)f_m}}{8s^2 J\omega^2}(1+2s)\omega\sin[(1+2s)\omega t - (2\alpha_\phi - \alpha_{(1-2s)f_1})]\} \tag{5.19}$$

Where m is the effective number of turns per phase winding of the stator.

Since $(1+2s)f_1$ is very close to $(1-2s)f_1$, the two additional electromotive forces are not much different, and the impedance is similar. It can be considered that the impedance relationship satisfies $z_1=z_2=z$. The resulting additional current can be expressed as:

$$i_{(1-2s)f_1} = \frac{e_{(1-2s)f_1}}{z} = -m\phi\frac{p\Delta T_{(1-2s)f_m}}{8s^2 J\omega^2 z}(1-2s)\omega\sin[(1-2s)\omega t - \alpha_{(1-2s)f_1}]\} \tag{5.20}$$

$$i_{(1+2s)f_1} = \frac{e_{(1+2s)f_1}}{z} = m\phi\frac{p\Delta T_{(1-2s)f_m}}{8s^2 J\omega^2 z}(1+2s)\omega\sin[(1+2s)\omega t - (2\alpha_\phi - \alpha_{(1-2s)f_1})]\} \tag{5.21}$$

From the above derivation and analysis, it can be known that when the rotor has an asymmetrical fault due to factors such as winding broken bars or end ring breakage, the stator winding will generate a current component $i_{(1-2s)f_1}$ which is $2s\omega$ lower than the grid frequency, and this component interacts with the air gap flux. Producing an alternating torque with a frequency of $2sf_1$, further causing the rotor to generate a continuously varying rotational speed

with a frequency of $2sf_1$, the alternating rotational speed reacting to the air gap magnetic field, generating an additional magnetic flux, and generating a frequency in the stator winding additional induced electromotive force and current of $(1\pm2s)f_1$. From this in-depth analysis, it can be seen that the current component of the stator winding with a frequency of $(1+2S)f_1$ will generate an induced electromotive force and current of $3sf_1$ in the rotor winding, which will appear in the stator magnetic potential under the action of the additional magnetic flux $(1-4s)f_1$. The frequency component will eventually induce an induced electromotive force and current at a frequency of $(1\pm4s)f_1$ in the stator winding under the influence of the $4sf_1$ rotational speed fluctuation, and so on, when the rotor fails. Characteristic frequency $(1\pm2ks)f_1$ The generation mechanism of the fl component.

In summary, the faulty state of the rotor can be diagnosed by monitoring the characteristic frequency component of the three-phase stator current $(1\pm2ks)f_1$, since the higher harmonic components of the fault signal are generated on the basis of low frequency harmonics. When the rotor has a slight fault, the higher harmonic components of the fault signal can be ignored, and the fault diagnosis of the rotor of the motor can be realized by analyzing the characteristic component of the fundamental wave $(1\pm2s)f_1$.

5.2   Stator interturn short circuit fault

The insulation part of the motor system is one of its weakest links, and its resistance to heat resistance, durability, mechanical strength and resistance to the environment is weak. Therefore, the insulation system is easily damaged by aging, wear, overheating, moisture, etc., resulting in short-circuit between the stator components and the phases. In addition, improper molding of the stator winding during the manufacturing process and improper operation of the transposition process will also cause a short circuit between turns. When the number of coils short-circuited between turns is small, it has little effect on the normal operation state of the motor, but as the

temperature at the short-circuit increases, it is easy to further cause damage to the surrounding insulation layer, resulting in a more serious turn-to-turn short circuit, even Serious faults such as phase-to-phase short-circuit and single-phase short-circuit occur.

When a single-phase inter-turn short-circuit fault occurs in the stator winding of the motor, the three-phase symmetrical winding parameters (such as impedance) change under normal conditions, resulting in three-phase asymmetry. At this time, the air gap magnetic potential generated by the stator winding is changed from a normal circular shape to an ellipse, whereby the magnetic potential components $\overrightarrow{F_{11}}$ and $\overrightarrow{F_{12}}$ having opposite directions and the same rotational speed can be decomposed. These two components induce two potentials with the same frequency and opposite phase sequence in the stator winding, and generate corresponding positive sequence current components and negative sequence current components. The negative sequence current component at this time is the fault characteristic signal.

At present, the methods for the diagnosis of stator turn-to-turn short-circuit faults proposed by scholars are generally based on the stator current signal. The parameters of the parameters mainly include the stator current negative sequence component method (detecting the change of the negative sequence component in the stator current), the stator three-phase current phase difference method (detecting the phase difference between the three-phase currents before and after the fault), and the stator current harmonic component method. (Detecting stator current harmonic frequency), etc., but the above methods are affected by motor load and input voltage imbalance, and need to be improved.

5.3   AC motor modeling and simulation

The establishment of the model is the necessary way to carry out mathematical analysis, theoretical research and law prediction, and the mathematical or physical model provides

theoretical support for the establishment of the simulation model. Establishing an appropriate model is of great significance to ensure the simplicity and clarity of data analysis and solution. Appropriate parameter selection plays an important role in exploring the feature law and fault identification. This section verifies the effectiveness of the current signal as a fault feature through coordinate transformation, theoretical calculation and simulation, and provides an important basis for subsequent analysis.

5.3.1 Establishment of mathematical model

The mathematical model of AC three-phase asynchronous motor has the characteristics of multivariable, nonlinear and high order. Usually when analyzing its mathematical model, the following assumptions are made to simplify the establishment of the model.

(1) The three-phase windings are symmetrical, and the magnetomotive force generated is sinusoidal around the air gap when the space is different from each other by 120 degrees;

(2) Ignoring the saturation of the magnetic circuit, the self-inductance and mutual inductance of each winding are linear;

(3) ignore the core loss;

(4) The influence of frequency and temperature changes on the winding resistance is not considered.

Consider the above assumptions, establish a simplified mathematical model of the AC asynchronous motor, as shown in equation (5.22)

$$\begin{cases} T_e = T_m + \dfrac{J}{p}\dfrac{\mathrm{d}\omega}{\mathrm{d}t} + \dfrac{D}{p}\omega + \dfrac{K}{p}\theta \\[2mm] U_a = E_a + R_a I_a + L_a \dfrac{\mathrm{d}I_a}{\mathrm{d}t} \\[2mm] E_a = C_e\omega \\[2mm] T_e = C_m I_a \end{cases} \tag{5.22}$$

Where T_e is the electromagnetic torque, T_m is the load torque, J is the moment of inertia of the unit, p is the pole number of the motor, D is the torque damping coefficient proportional to the speed, K is the torsional elastic torque coefficient. U_a, R_a, I_a, L_a all are motor stator parameters, Ea is the induced electromotive force generated by the cutting of the magnetic field for the armature rotation, C_e is the electromotive force constant, C_m is the torque constant, and ϑ is the mechanical torsion angle.

The first equation in equation (5.22) is the equation of motion of the transmission system, which represents the torque balance relationship of the AC motor under dynamic conditions. In general, for a constant torque load with D=0, K= 0, this equation can be simplified as shown in (5.23).

$$T_e = T_m + \frac{J}{p}\frac{\mathrm{d}\omega}{\mathrm{d}t} \tag{5.23}$$

It can be seen that when there is disturbance in the load torque T_m, the torque equation must be balanced by the change of the rotational speed.

The second equation in equation (5.22) is the voltage balance equation. Generally speaking, when the equipment is running, the power supply capacity provided by the grid is large, and the fluctuation due to the load is small, so the influence of the load change on the stator voltage can be ignored. When the rotational speed is changed by the disturbance of the load torque, the equilibrium relationship of the voltage equation is satisfied by the stator current response. When electrical or mechanical faults occur in components in the rotor system, torsional vibrations of

the shafting and stator current oscillations are often generated, and torsional vibrations cause changes in the air gap of the AC motor's spatial magnetic field, resulting in changes in magnetic flux and induced electromotive force. Eventually it causes a change in the stator current.

5.3.2 Establishment of simulation model

According to the above theory, a multi-loop mathematical model of the asynchronous motor can be established in the three-phase stationary coordinate system ABC and the three-phase rotating coordinate system abc, respectively. It can be seen from the analysis that the stator current signal of the asynchronous motor can be used as the main signal basis for motor fault diagnosis, tracking the change of the stator current signal in real time, and realizing the online monitoring and fault diagnosis of the motor state. However, it is very difficult to directly solve the mathematical model of a three-phase asynchronous motor. To this end, the mathematical model in the three-phase coordinate system can be transformed into a two-phase coordinate system by auxiliary coordinate transformation, and the above model is simplified by using this identity transformation.

The two-phase coordinate system includes an α-β coordinate system and a d-q coordinate system. The α-β coordinate system is a two-phase orthogonal and stationary coordinate system. Since the two-phase coordinate axes are perpendicular to each other, there is no electromagnetic coincidence between the two-phase windings. The d-q coordinate system is a two-phase orthogonal rotating coordinate system obtained by rotating the α-β coordinate system at an arbitrary angle, and is a time-varying coordinate system. When one of the coordinate axes in the d-q coordinate system is in the same direction as the rotor flux, the coordinate system rotates at a synchronous speed, which is a time-invariant system. In this section, based on the α-β coordinate transformation, the mathematical model of the three-phase asynchronous motor in the d-q coordinate system and the corresponding simulation model are established.

5.3.2.1　Basic principle of coordinate transformation

(1) α-β coordinate system (two-phase synchronous stationary coordinate system)

The model transformation from the three-phase abc system to the α-β system is as shown in (5.24):

$$\begin{bmatrix} X_\alpha \\ X_\beta \end{bmatrix} = \sqrt{\frac{2}{3}} \begin{bmatrix} 1 & -\frac{1}{2} & -\frac{1}{2} \\ 0 & \frac{\sqrt{3}}{2} & -\frac{\sqrt{3}}{2} \end{bmatrix} \begin{bmatrix} X_a \\ X_b \\ X_c \end{bmatrix}$$

(5.24)

That is, the current relationship of the abc system to the system α-β is as shown in equation (5.25):

$$\begin{cases} i_\alpha = \sqrt{\frac{2}{3}} i_a - \sqrt{\frac{1}{6}} i_b - \sqrt{\frac{1}{6}} i_c \\ i_\beta = \sqrt{\frac{1}{2}} i_b - \sqrt{\frac{1}{2}} i_c \end{cases}$$

(5.25)

In the α-β system, the voltage equation of the motor is shown in equation (5.26), where (1) and (2) are the stator model voltage equation, (3) and (4) are the rotor model voltage equation.

$$\begin{cases} u_{\alpha 1} = r_1 i_{\alpha 1} + \Delta \psi_{\alpha 1} & (1) \\ u_{\beta 1} = r_1 i_{\beta 1} + \Delta \psi_{\beta 1} & (2) \\ u_{\alpha 2} = r_2 i_{\alpha 2} + \Delta \psi_{\alpha 2} + \psi_{\beta 2} \omega_r & (3) \\ u_{\beta 2} = r_2 i_{\beta 2} + \Delta \psi_{\beta 2} + \psi_{\alpha 2} \omega_r & (4) \end{cases}$$

(5.26)

In the α-β system, the flux linkage equation of the motor is expressed by equation (5.27), where (1) and (2) are the stator model flux linkage equation, (3) and (4) are the rotor model flux linkage equation.

$$
\begin{cases}
\psi_{\alpha1} = L_1 i_{\alpha1} + L_m i_{\alpha2} & (1) \\
\psi_{\beta1} = L_1 i_{\beta1} + L_m i_{\beta2} & (2) \\
\psi_{\alpha2} = L_2 i_{\alpha2} + L_m i_{\alpha1} & (3) \\
\psi_{\beta2} = L_2 i_{\beta2} + L_m i_{\beta1} & (4)
\end{cases}
$$

$$(5.27)$$

The electromagnetic torque and load torque equations are shown in equation (5.28):

$$
\begin{cases}
T_e = p L_m (i_{\beta1} i_{\alpha2} - i_{\beta2} i_{\alpha1}) \\
T_e = T_m + \dfrac{J}{p}\dfrac{d\omega}{dt}
\end{cases}
$$

$$(5.28)$$

Among them ω_r is rotor rotational angular velocity, r_1 and L_1 are stator winding resistance and self-inductance, r_2 and L_2 are rotor winding resistance and mutual inductance, L_m is stator and rotor winding mutual inductance, p is magnetic pole pair, $\triangle$ is differential operator.

(2) d-q coordinate system (two-phase synchronous rotating coordinate system)

The transformation of the abc three-phase coordinate system to the d-q coordinate system can only be rotated by an arbitrary angle of the ap coordinate system (rotating at the speed of ωt), that is, multiplied by the rotating coordinate system on the basis of α-β coordinate transformation) The equation of transformation (5.29) is obtained.

$$
\begin{bmatrix} X_d \\ X_q \end{bmatrix} = \sqrt{\frac{2}{3}}
\begin{bmatrix} \cos\theta & \sin\theta \\ -\sin\theta & \cos\theta \end{bmatrix}
\begin{bmatrix} 1 & -\frac{1}{2} & -\frac{1}{2} \\ 0 & \frac{\sqrt{3}}{2} & -\frac{\sqrt{3}}{2} \end{bmatrix}
\begin{bmatrix} X_a \\ X_b \\ X_c \end{bmatrix}
$$

$$
= \sqrt{\frac{2}{3}}
\begin{bmatrix} \cos\theta & \cos(\theta-\frac{2}{3}\pi) & \cos(\theta+\frac{2}{3}\pi) \\ -\sin\theta & -\sin(\theta-\frac{2}{3}\pi) & -\sin(\theta+\frac{2}{3}\pi) \end{bmatrix}
\begin{bmatrix} X_a \\ X_b \\ X_c \end{bmatrix}
$$

$$(5.29)$$

The voltage equation of the motor in the d-q coordinate system is shown in equation (5.30), where (1) and (2) are the stator model voltage equation, (3) and (4) are the rotor model voltage equation.

$$\begin{cases} u_{d1}=r_1 i_{d1}+\Delta\psi_{d1}-\psi_{q1}\omega_1 & (1) \\ u_{q1}=r_1 i_{q1}+\Delta\psi_{q1}+\psi_{d1}\omega_1 & (2) \\ u_{d2}=r_2 i_{d2}+\Delta\psi_{d2}-\psi_{q2}(\omega_1-\omega_r) & (3) \\ u_{q2}=r_2 i_{q2}+\Delta\psi_{q2}+\psi_{d2}(\omega_1-\omega_r) & (4) \end{cases}$$

(5.30)

The flux linkage equation of the motor in the d-q coordinate system is shown in equation (5.31), where (1) (2) is the stator model flux linkage equation, and (3) (4) is the rotor model flux linkage equation.

$$\begin{cases} \psi_{d1} = L_1 i_{d1} + L_m i_{d2} & (1) \\ \psi_{q1} = L_1 i_{q1} + L_m i_{q2} & (2) \\ \psi_{d2} = L_2 i_{d2} + L_m i_{d1} & (3) \\ \psi_{q2} = L_2 i_{q2} + L_m i_{q1} & (4) \end{cases}$$

(5.31)

The electromagnetic torque and load torque equations are shown in equation (5.32):

$$\begin{cases} T_e = pL_m(i_{q1}i_{d2} - i_{q2}i_{d1}) \\ T_e = T_m + \dfrac{J}{p}\dfrac{d\omega}{dt} \end{cases}$$

(5.32)

During the model building process, the d-axis is consistent with the direction of the total flux linkage of the motor rotor ψ_2, and the projection of the rotor flux linkage on the q-axis is 0, as $\psi_{d2}=\psi_2$, $\psi_{q2}=0$, then the voltage in the above mathematical model And the flux linkage equation can be simplified as shown in equation (5.33).

$$
\begin{cases}
u_{d1} = r_1 i_{d1} + \Delta\psi_{d1} - \psi_{q1}\omega_1 & (1) \\
u_{q1} = r_1 i_{q1} + \Delta\psi_{q1} + \psi_{d1}\omega_1 & (2) \\
u_{d2} = r_2 i_{d2} + \Delta\psi_2 & (3) \\
u_{q2} = r_2 i_{q2} + \psi_2(\omega_1 - \omega_r) & (4) \\
\psi_{d1} = L_1 i_{d1} + L_m i_{d2} & (5) \\
\psi_{q1} = L_1 i_{q1} + L_m i_{q2} & (6) \\
\psi_2 = L_2 i_{d2} + L_m i_{d1} & (7) \\
0 = L_2 i_{q2} + L_m i_{q1} & (8)
\end{cases}
\tag{5.33}
$$

From equations (5.33) and (7):

$$
i_{d2} = L_2^{-1}(\psi_2 - L_m i_{d1})
\tag{5.34}
$$

From equations (5.34) and (8):

$$
i_{q2} = -L_2^{-1} L_m i_{q1}
\tag{5.35}
$$

The eight equations in equation (5.33) are transformed to obtain a matrix expression of the motor stator and rotor voltage equation.

$$
\begin{bmatrix} U_{d1} \\ U_{q1} \\ U_{d2} \\ U_{q2} \end{bmatrix} = \begin{bmatrix} U_{d1} \\ U_{q1} \\ 0 \\ 0 \end{bmatrix} = \begin{bmatrix} r_1 + \Delta L_1 & -\omega_1 L_1 & \Delta L_m & -\omega_1 L_m \\ \omega_1 L_1 & r_1 + \Delta L_1 & \omega_1 L_m & \Delta L_m \\ \Delta L_m & 0 & r_2 + \Delta L_2 & 0 \\ (\omega_1 - \omega_r)L_m & 0 & (\omega_1 - \omega_r)L_2 & r_2 \end{bmatrix} \begin{bmatrix} i_{d1} \\ i_{q1} \\ i_{d2} \\ i_{q2} \end{bmatrix}
\tag{5.36}
$$

Substituting (5.34) (5.35) into the third and fourth expressions of the matrix equation shown in (5.36), we obtain:

$$
(r_2 L_2^{-1} + \Delta)\psi_2 = r_2 L_2^{-1} L_m i_{d1}
\tag{5.37}
$$

$$
i_{q1} = r_2^{-1} L_2 L_m^{-1}(\omega_1 - \omega_r)\psi_2
\tag{5.38}
$$

Substituting (5.34) (5.37) (5.38) into the first expression of the (5.36) matrix equation, we

obtain:

$$(R+\Delta L)i_{d1}=U_{d1}+\omega_1 L i_{q1}+A\psi_2 \tag{5.39}$$

Among them, $R=r_1+r_2(L_m^2/L_2^2)$, $A=L_m(r_2/L_2^2)$, $L=L_1-L_m^2/L_2$.

Substituting (5.34) (5.37) (5.38) into the first expression of the (5.36) matrix equation:

$$(r_1+\Delta L)i_{q1}=U_{q1}-\omega_1 L i_{d1}-B\omega_1\psi_2 \tag{5.40}$$

Among them $B=L_m L_2^{-1}$.

Substituting (5.34) (5.35) into (5.32), the electromagnetic torque and torque equation are:

$$T_e=pL_2^{-1}L_m\psi_2 i_{q1} \tag{5.41}$$

$$T_e-T_L=p^{-1}J\frac{\mathrm{d}\omega_r}{\mathrm{d}t} \tag{5.42}$$

5.3.3 Simulation model based on d-q coordinate system

Since the two-phase synchronous rotating coordinate system (d-q coordinate system) is obtained by rotational transformation of the two-phase synchronous stationary coordinate system (α-β coordinate system), that is, the α-β coordinate system is the state of the d-q coordinate system at a specific angle, so this section The simulation analysis of the fault states of the asynchronous motor is focused on the two-phase synchronous rotating coordinate system.

5.3.3.1   Establishment of simulation model

According to the electromagnetic relationship of the motor in equation (5.3.16)~(5.3.21), the mathematical model of the three-phase asynchronous motor in the d-q coordinate system is established in the MATLAB/Simulink environment. The model structure is shown in

Figure5.3.2.1. In the figure, the actual working condition of the asynchronous motor in two-phase rotating coordinate system is simulated. The input end is the motor working voltage U_d, U_q, load torque T_m and the stator angular speed ω_1; the output end is motor current i_d, i_q, rotor speed n and working load T_e.
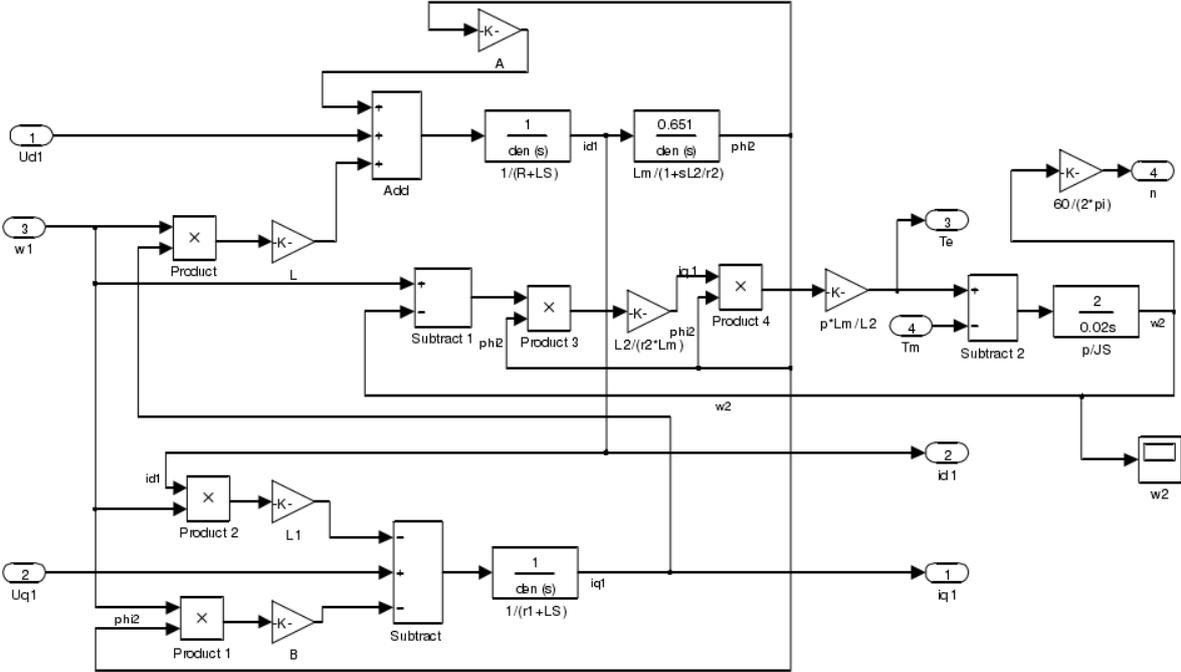

Figure 5.1 Model structure of asynchronous motor in d-q coordinate system.

Taking into account the three-phase voltage signal provided by the input terminal for the grid during the actual operation, the output is a three-phase current signal. Therefore, on the basis of Figure 3.1, the three-phase static voltage is set to the two-phase rotation voltage change at the input end. The conversion module is provided with a conversion module of two-phase rotating current to three-phase static current change at the output end, and the package model of the three-phase asynchronous motor simulation model shown in Fig 5.3.2.2 is obtained. In the figure, system is the package diagram of the motor system structure, and its internal structure is shown in Figure 5.3.2.3. Where change_voltage_system is the voltage conversion module change_current_system is the current conversion module, and d-q system is the package

structure of the model in Figure 5.2.3.1. The oscilloscope is used to observe the output

waveform result of the simulation data.
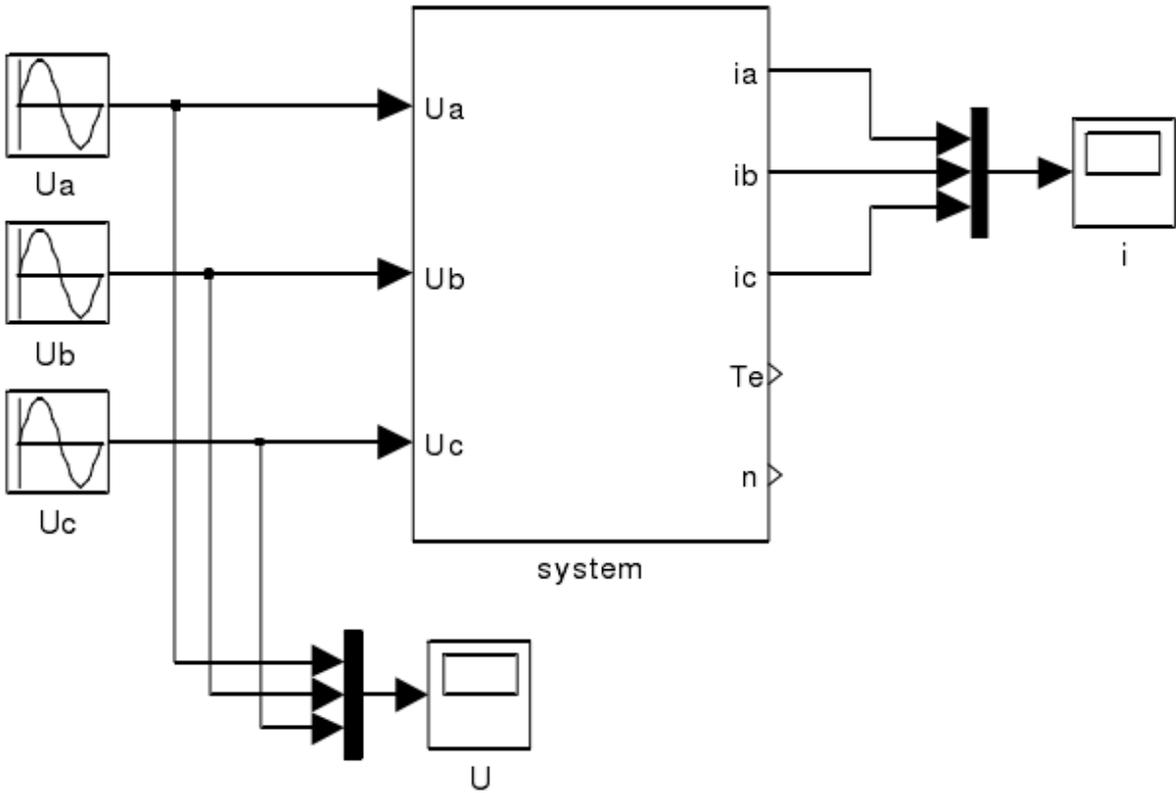
Figure 5.2 Asynchronous motor simulation model package diagram.
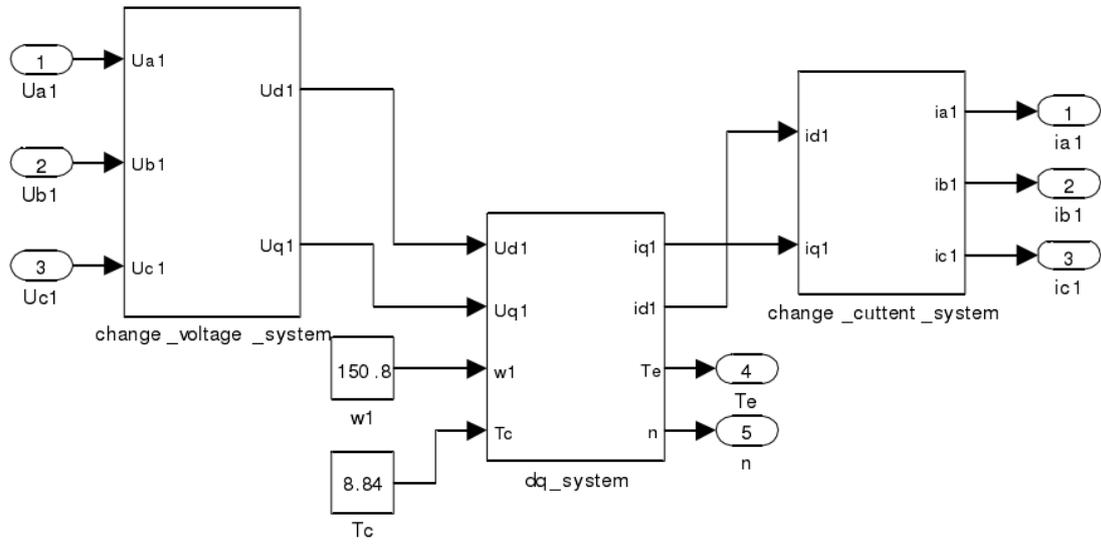
Figure 5.3 system model internal structure.

5.3.3.2   Input parameter settings

The basic parameters entered in the simulation model are set as follows:

Table 5-1 The basic parameters entered in the simulation model

Motor pole pair	$P=2$
Power frequency	$f=50HZ$
Input voltage	$U_a=220\sin(2\pi ft), U_b=220\sin(2\pi ft-2/3\pi)$, $U_c=220\sin(2\pi ft+2/3\pi)$
Load torque	$T_m=8.84Nm$
Stator winding internal resistance	$r_1=4.26\Omega$
Rotor winding internal resistance	$r_2=3.24\Omega$
Stator self-inductance coefficient	$L_1=0.666H$
Rotor self-inductance coefficient	$L_2=0.670H$
Stator and rotor mutual inductance	$L_m=0.651H$
System moment of inertia	$J=0.02kg.m^2$
Rotation speed	$n_1=1440r/min$
Rotor angular velocity	$\omega_1=150.8rad/min$

5.3.3.3   Simulation environment settings

Simulink simulation environment provides a variety of solvers (Solver, that is, the solution algorithm), because the asynchronous motor model contains nonlinear factors, so in the simulation process using Fixed-step algorithm. In the simulation process, it was found that

different solvers and step sizes had different influences on the simulation results. In order to make the algorithm more effective, the following parameters were set through multiple experiments: ode4 was selected for the solver (based on the fourth-order runge-kutta formula), 0.1 millisecond for the simulation step, and 0.5 seconds for the simulation time.

5.3.3.4 Simulation result

The output results obtained under the above simulation conditions are shown in figure 5.3.2.4 and figure 5.2.3.5. Figure 5.2.3.4 shows the output three-phase current signal. It can be seen that the starting current of the motor fluctuates greatly and basically reaches the steady state at 0.ls. Figure 3.2.3.5 shows the output results of torque T_e and rotation speed n. At steady state, the motor speed reaches 1424rad/min and the torque fluctuates at 8.84nm, which is consistent with the actual motor model.
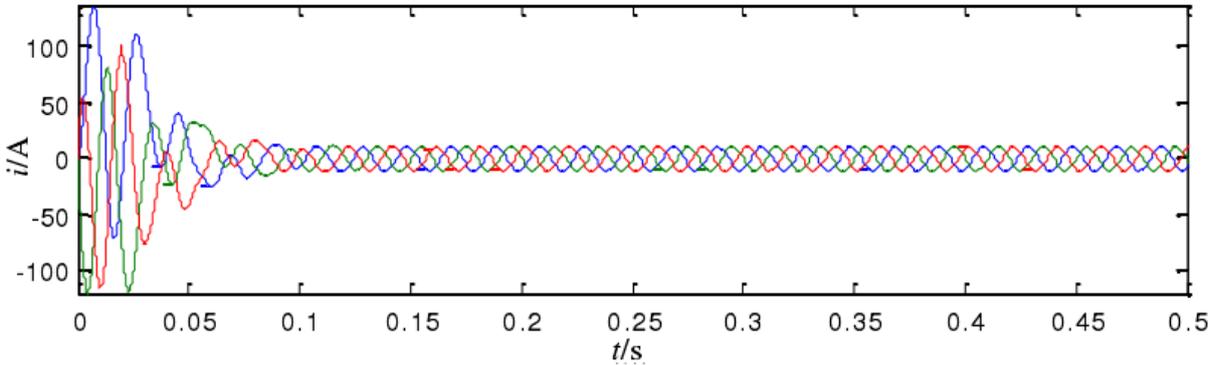
Figure 5.4 Stator three - phase current simulation signal
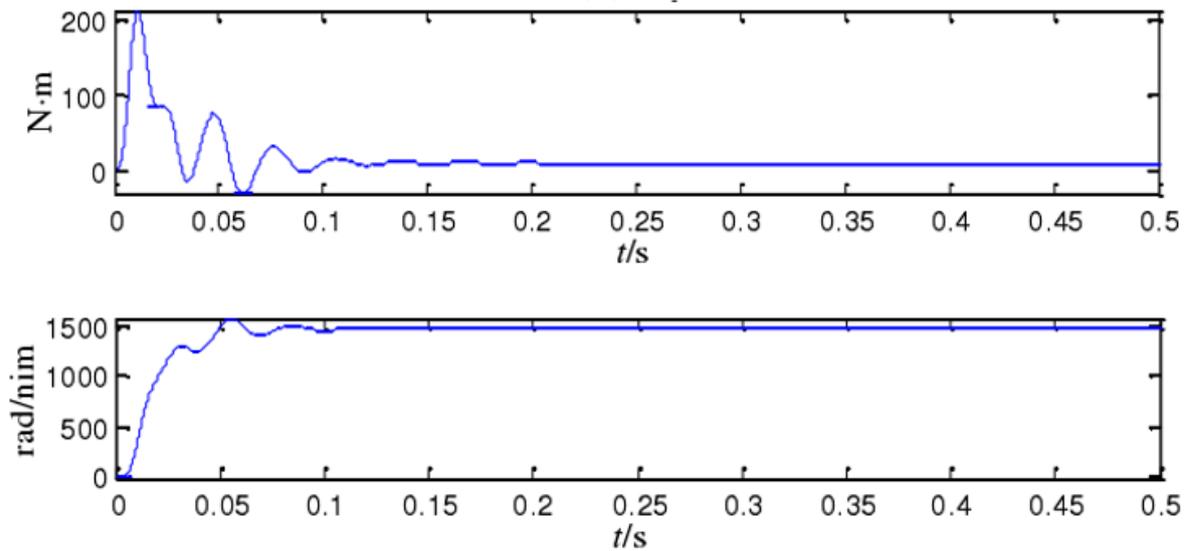
Figure 5.5 Torque and speed simulation results

In this section, the simulation model of system mathematical function is established according to the dynamic equation of asynchronous motor. The relationship between parameters in the mathematical model of asynchronous motor is clearly expressed in the model diagram, and the conversion relationship between three-phase coordinate system and two-phase coordinate system is directly reflected.

5.3.4 simulation model based on module library

In order to verify the validity of the above model, this section establishes the AC asynchronous motor simulation model based on the power system module set (SimPowerSystems) provided by MATLAB/Simulink, simulates the normal motor, and obtains the time domain signals such as current, torque and speed.

5.3.4.1   Input parameter setting

It is shown in figure 5.6 that, Asynchronous Machine SI Units is squirrel-cage asynchronous motor from machines module library. The parameters are set as follow table:
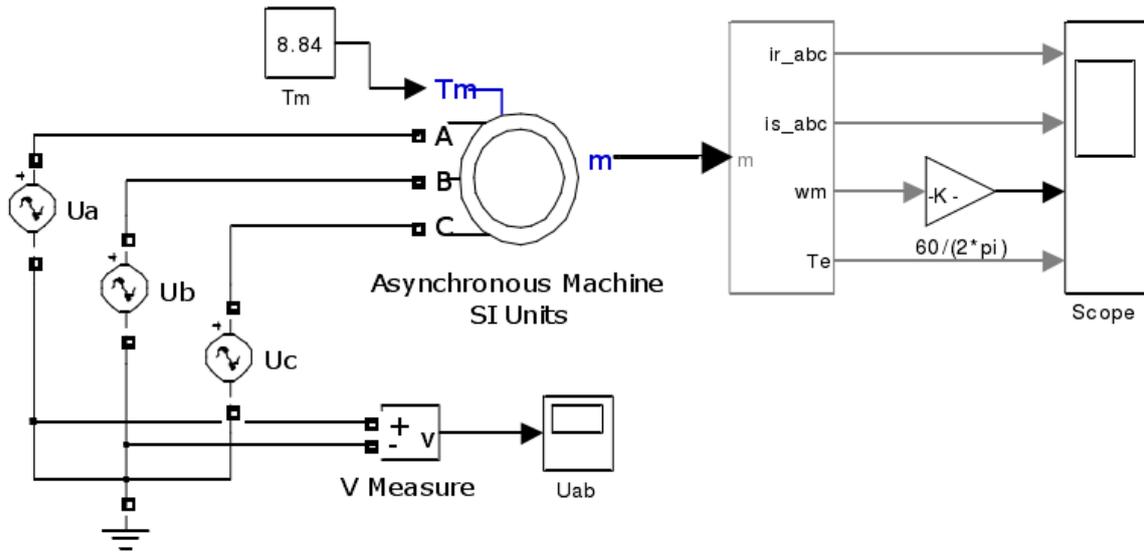
Figure 5.6 Simulation model of asynchronous motor based on module library

Table 5-2 The basic parameters entered in the simulation model

Motor pole pair	P=2
Power frequency	f=50HZ
Input voltage	U_a=220sin(2πft),U_b=220sin(2πft-2/3π), U_c=220sin(2πft+2/3π)
Load torque	T_m=8.84Nm
Stator winding internal resistance	r_1=0.435Ω
Rotor winding internal resistance	r_2=0.816Ω
Stator self-inductance coefficient	L_1=2*10⁻³H
Rotor self-inductance coefficient	L_2=2*10⁻³H

Stator and rotor mutual inductance	$L_m=6.931*10^{-2}H$
System moment of inertia	$J=0.02kg.m^2$
Rotation speed	$n_1=1440r/min$
Friction coefficient	$F=0N.m.s$
Simulation step	$0.1ms$
Simulation time	$5s$

5.3.4.2   Simulation results and spectrum analysis

The results of three-phase stator current signal, torque and rotation speed under normal state as shown in figure 5.7 are obtained by simulation, and the simulation waveform within 0~0.5s is drawn in the figure. As can be seen from the figure, the motor generated A large starting current and starting torque during the starting process, and the system tended to stabilize after 0.15s. At this time, the stator current fluctuated around 10.6A, and the speed n=1475rad/min was close to the rated speed, and the torque fluctuated around 8.84Nm at the rated load. The simulation results are consistent with the theoretical operation results of the motor model.
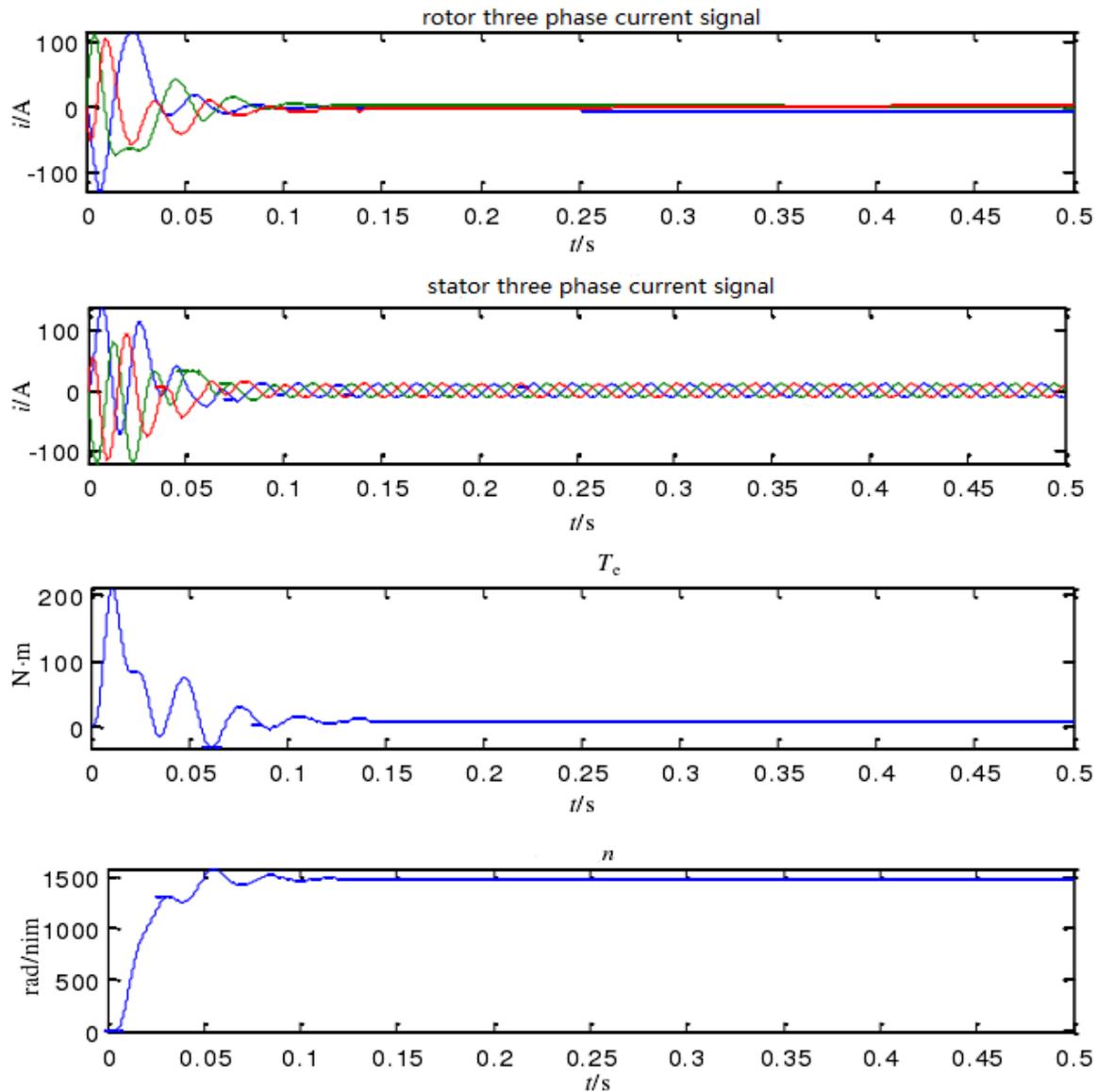
Figure 5.7 Results of normal time domain simulation

Based on the stator current signal in figure 5.7, fast Fourier transform (FFT) is adopted to conduct spectrum analysis on it, and the spectrum result of a-phase current signal shown in figure 5.8 is obtained. The working frequency (f=50.1031HZ) of the motor under normal state is calculated through the program, which is consistent with the theoretical value of power grid frequency.
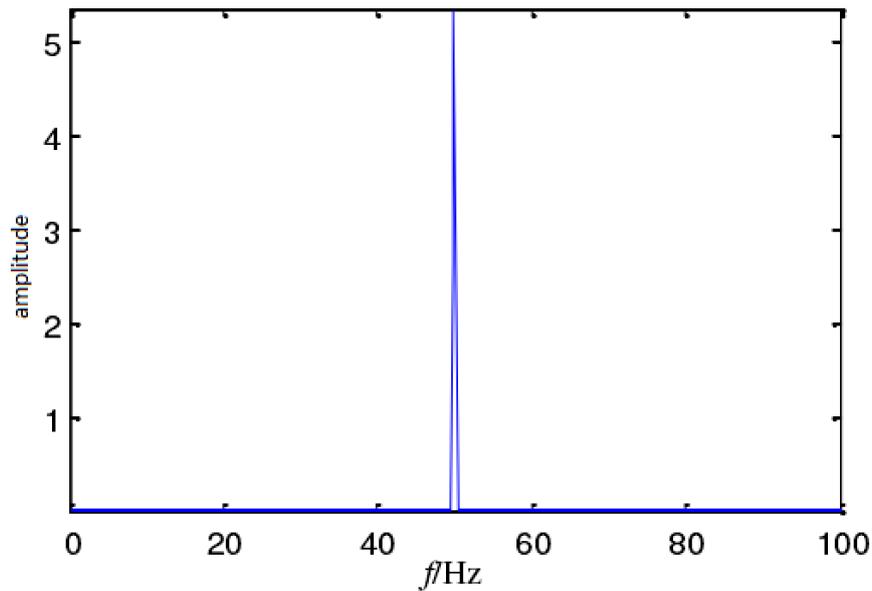
Figure 5.8 Normal a-phase stator current spectrum

By comparing the simulation time domain waveform of the above two models, it can be seen that the simulation results of the two models are basically consistent, which can verify the correctness and effectiveness of the simulation model established above based on the mathematical equation of asynchronous motor dynamics.

5.4   Fault characteristic signal extraction and simulation analysis

With the increasing complexity of power equipment system, fault signs often show diversified characteristics, and are easily drowned by electromagnetic interference, vibration noise and other factors. The motor usually contains a large amount of information unrelated to the characteristic signal. In order to detect the motor fault, it is necessary to extract the fault characteristics from the large fundamental frequency background signals through different feature extraction algorithms to carry out state recognition. Starting from the basis of signal time and frequency analysis, this chapter conducts simulation analysis of fixed and rotor fault

states, and analyzes fault signals through the Park vector transformation method and Amplitude adjustment method.

5.4.1 Park vector transformation method

Park vector method converts stator three-phase current into a two-phase synchronous static coordinate system and obtains current components i_α and i_β. The vector trajectory formed by them realizes the graphical identification of motor faults. This method relies on the spectrum component characteristics at the double frequency, where the amplitude of the spectrum component is directly related to the degree of asymmetry of the motor winding. According to the model of asynchronous motor established in chapter 5.3, the conversion relationship is shown in equation (5.43).

$$\begin{cases} i_\alpha = \sqrt{\dfrac{2}{3}} i_a - \sqrt{\dfrac{1}{6}} i_b - \sqrt{\dfrac{1}{6}} i_c \\ i_\beta = \sqrt{\dfrac{1}{2}} i_b - \sqrt{\dfrac{1}{2}} i_c \end{cases}$$

(5.43)

Set the steady-state stator current of the motor running under normal state as:

$$\begin{cases} i_a = \sqrt{2} I \sin(\omega t + \varphi) \\ i_b = \sqrt{2} I \sin(\omega t + \varphi - 120°) \\ i_a = \sqrt{2} I \sin(\omega t + \varphi + 120°) \end{cases}$$

(5.44)

Substitute into equation (5.43), and after simplification, the two-phase current component is:

$$\begin{cases} i_\alpha = \sqrt{3} I \sin(\omega t + \varphi) \\ i_\beta = -\sqrt{3} I \cos(\omega t + \varphi) \end{cases}$$

(5.45)

As can be seen from equation (5.45), for an ideal asynchronous motor, its current vector trajectory is circular. According to the theoretical analysis and three chapters of the second chapter of the simulation result shows that when the motor stator winding interturn short circuit,

and the asymmetric fault such as short circuit, the three phase stator current will produce negative sequence component, and with the increase of the degree of fault, the change of the negative sequence component is more and more big, the result will directly lead to the current vector trajectory into ellipse, mainly reflects the degree of fault on the elliptical axle change and the deflection Angle. The length of the long axis of the ellipse is proportional to the sum of the amplitudes of the positive and negative sequence current components, and the length of the short axis is proportional to the difference between the amplitudes of the two components. While Park vector module $\left|i_\alpha^2 + i_\beta^2\right|$ contains dc and ac components directly related to motor short circuit fault.

Due to the relatively low sensitivity of graphics to early fault identification, the extended Park vector method was developed. Its essence is to carry out spectrum analysis of vector model $\left|i_\alpha^2 + i_\beta^2\right|$ of two-phase current components. Its advantage is to convert the fundamental wave component of three-phase current into the dc component, so as to highlight the side frequency component $2ksf_1$ of rotor bar breaking, end ring breaking and other faults, and distinguish the fault characteristic frequency from the power supply fundamental frequency.

5.4.2 Analysis of stator and rotor fault simulation signals

Since the amplitude of the fundamental wave component of the three-phase current is relatively large compared with the characteristic component, and spectrum leakage will occur when the signal is truncated. If the signal is directly extended Park vector spectrum analysis at this time, the dc component will easily leak to other spectrum components, especially the low-frequency component, thus affecting the accuracy of the low-frequency component. In this paper, linear trend of time domain data is removed before frequency domain analysis, and time domain window is added. From the simulation results, it can be seen that this method has obvious effect on removing dc components in frequency domain.

Transfer stator three-phase current to stationary two-phase coordinate system and draw vector trajectories of current component i_α and i_β. Figure 5.9(a) is the vector diagram of two-phase current under normal state, and the trajectory is circular. Figure 5.9(b) is the spectrum diagram obtained by spectral analysis of $\left| i_\alpha^2 + i_\beta^2 \right|$. It can be seen that the fundamental wave component has been changed into the DC component filter. Figure 5.10(a)~(d) and figure 5.11(a)~(d) are obtained by respectively performing the above operations for rotor and stator asymmetric faults of different degrees. It can be seen that the stator current vector trajectories become wider and wider, and the number of side frequency components and amplitude in the spectrum diagram increase with the aggravating of the asymmetric fault degree of the rotor. When there is a stator asymmetry fault of the motor, its vector trajectory turns into an ellipse, and the ratio of the major and minor axes of the ellipse increases with the increase of the fault degree. In the actual operation of motor equipment, stator three-phase current signal is seriously affected by electromagnetic interference, noise, field environment, sensor acquisition equipment and other factors, which will lead to the generation of signal error and waveform deviation, make the current vector track appear obvious deformation and affect the judgment of motor state. Therefore, the time-domain characteristic of Park vector transformation cannot be an effective characteristic quantity for motor state detection.
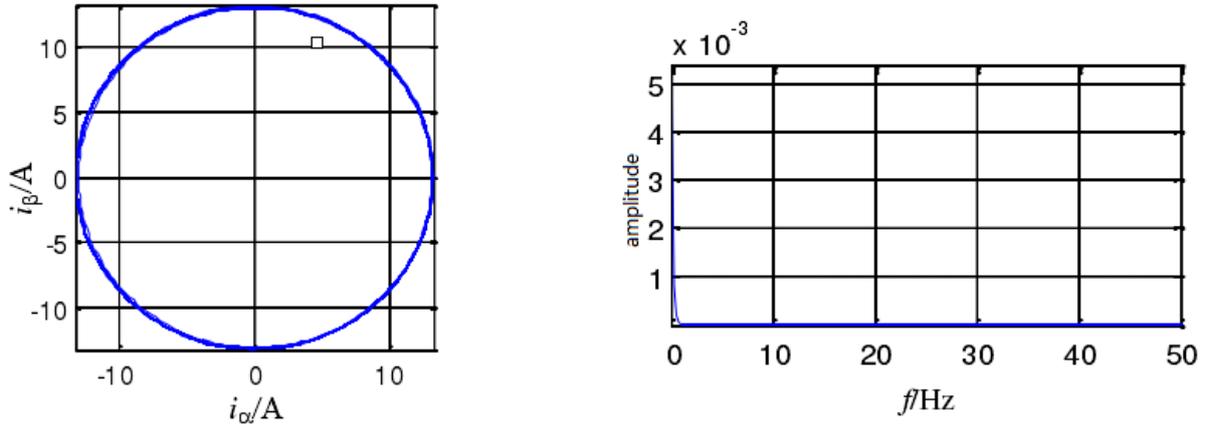
Figure 5.9 Stator current vector and spectrum during normal operation
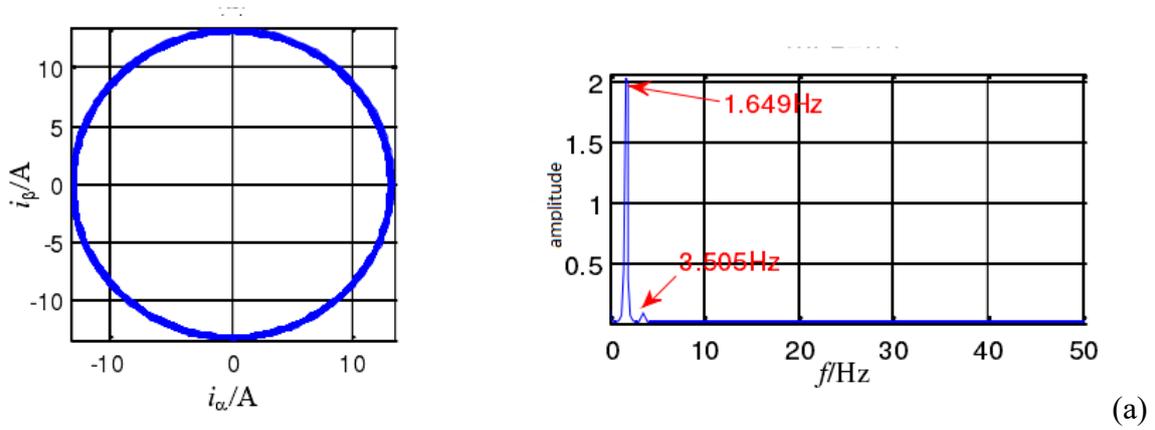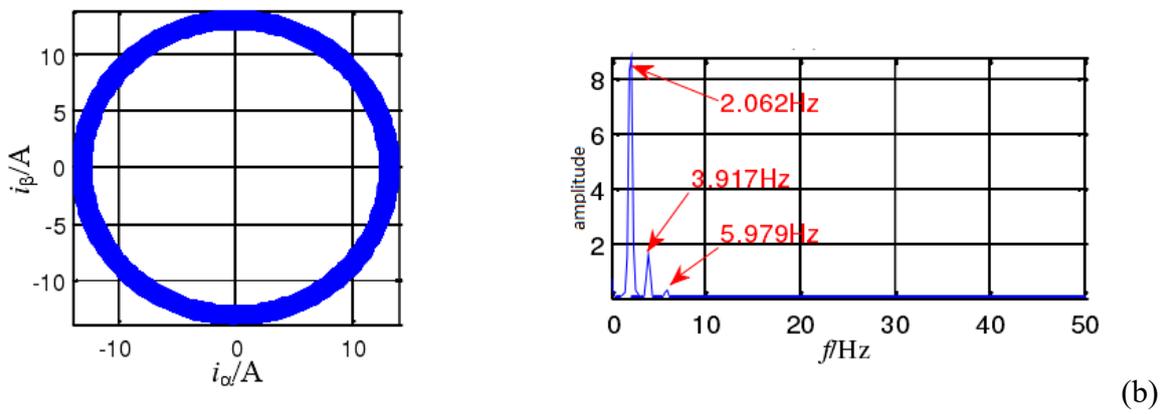
(a)

rotor fault resistance R=0.1Ω

(b)

rotor fault resistance R=0.5Ω

(c)

rotor fault resistance R=1Ω

·(d)·
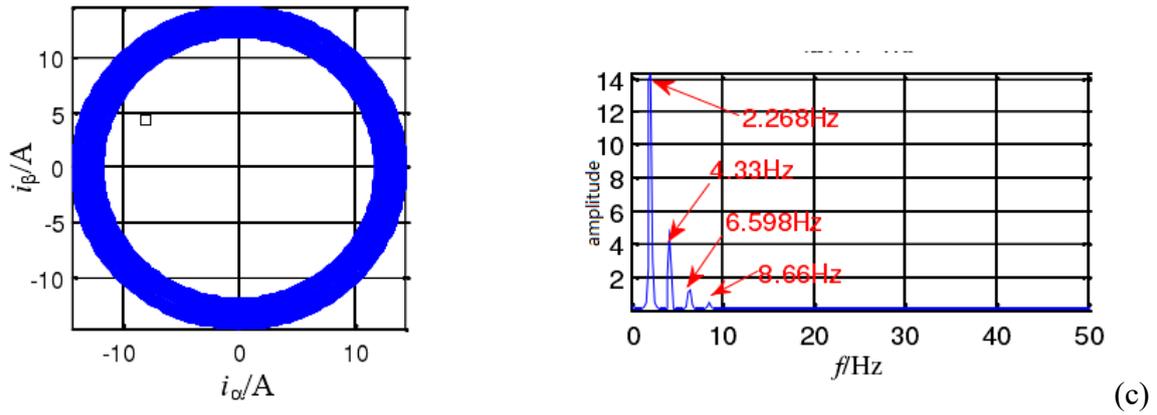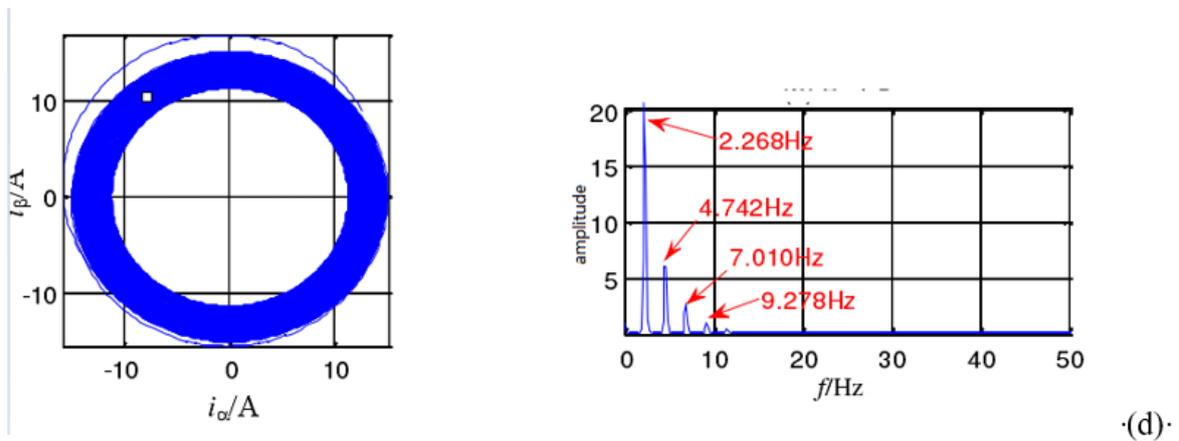
rotor·fault·resistance·R=1.5Ω¶

Figure 5.10 Rotor fault current vector and spectrum at different degrees

(a)
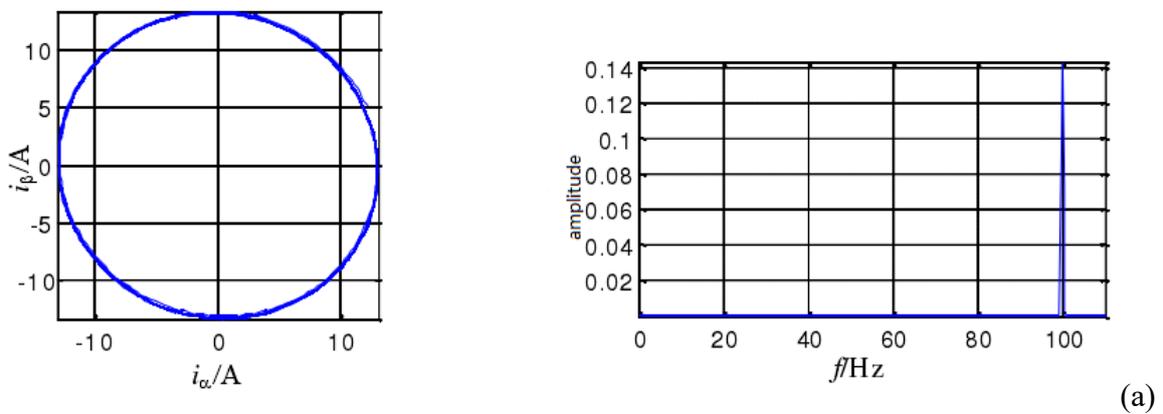
stator fault resistance R=0.1Ω
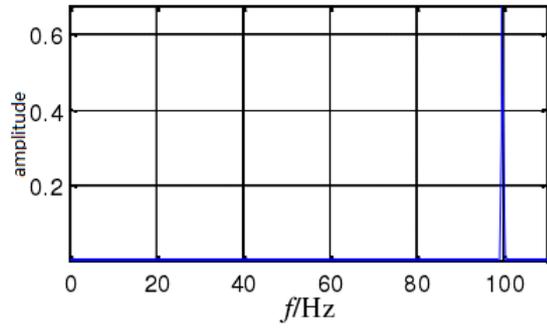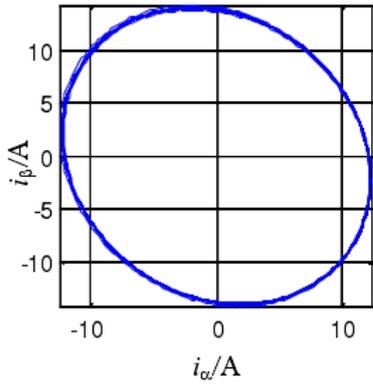
(b)

stator fault resistance R=0.5Ω
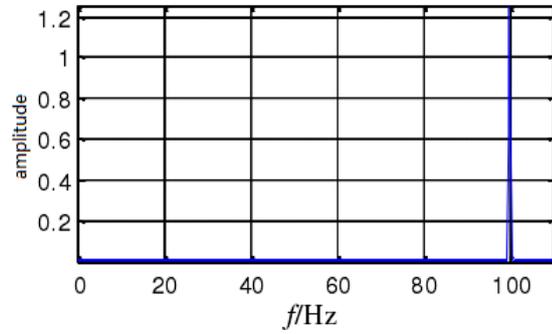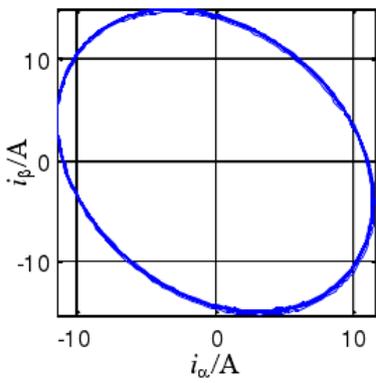
(c)

stator fault resistance R=1Ω
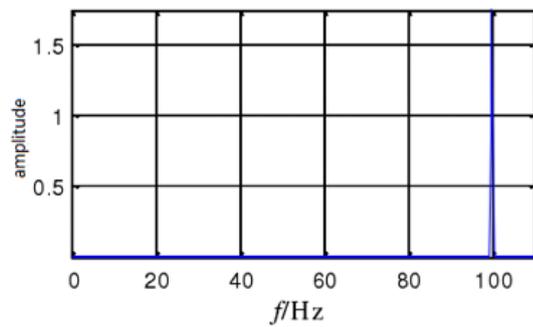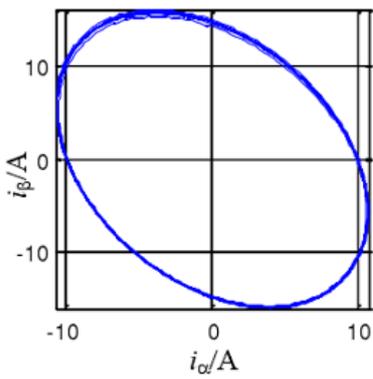
(d)·

stator·fault·resistance·R=1.5Ω¶

Figure 5.11 Stator fault current vector and spectrum at different degrees

5.4.3 An improved fault diagnosis algorithm based on vector transformation of stator and rotor

5.4.3.1 Fundamental analysis

When motor, rotor asymmetric composite fault occurring at the same time, due to the presence of the stator failure will cause the change of the three phase current phase signal, to convert current signal to the synchronous coordinate system, recycling Park vector transform two kinds of fault state can be reflected on the vector frequency spectrum, can distinguish between stator composite fault diagnosis.

Assuming that asynchronous motors have both stator turn-to-turn short-circuit fault and rotor bar breaking fault, then the stator three-phase current can be expressed as:

$$i_a = I_{p1}\cos(2\pi f_1 t - \alpha_p) + I_{n1}\cos(2\pi f_1 t - \alpha_n)$$
$$+ \sum_{k=1}^{\infty}\{I_{bpk}\cos[(1-2ks)2\pi f_1 t - \beta_{bpk}] + I_{bnk}\cos[(1+2ks)2\pi f_1 t - \beta_{bnk}]\} \tag{5.46}$$

$$i_b = I_{p1}\cos(2\pi f_1 t - \alpha_p - \frac{2}{3}\pi) + I_{n1}\cos(2\pi f_1 t - \alpha_n + \frac{2}{3}\pi)$$
$$+ \sum_{k=1}^{\infty}\{I_{bpk}\cos[(1-2ks)2\pi f_1 t - \beta_{bpk} - \frac{2}{3}\pi] + I_{bnk}\cos[(1+2ks)2\pi f_1 t - \beta_{bnk} - \frac{2}{3}\pi]\} \tag{5.47}$$

$$i_c = I_{p1}\cos(2\pi f_1 t - \alpha_p + \frac{2}{3}\pi) + I_{n1}\cos(2\pi f_1 t - \alpha_n - \frac{2}{3}\pi)$$
$$+ \sum_{k=1}^{\infty}\{I_{bpk}\cos[(1-2ks)2\pi f_1 t - \beta_{bpk} + \frac{2}{3}\pi] + I_{bnk}\cos[(1+2ks)2\pi f_1 t - \beta_{bnk} + \frac{2}{3}\pi]\} \tag{5.48}$$

Where, I_{p1} and I_{n1} are the positive and negative sequence amplitudes of the fundamental wave components of the stator current. I_{bpk} and I_{bnk} are the k-order harmonic amplitude of rotor splinters at the characteristic frequencies $(1-2ks)f_1$ and $(1+2ks)f_1$. α_p, α_n, β_{bpk} and β_{bnk} are the initial phases of the above current components

According to the rotation coordinate transformation principle described in chapter 5.3, the

three-phase current is converted to the synchronous rotation coordinate system d-q, and the included angle $\vartheta=\omega_{1t}+\vartheta_0$ between axis d and stator a-phase winding, where ϑ_0 is the initial included Angle when t=0. The three-phase current is transformed into the following results after the synchronous rotation coordinate transformation of the two phases:

$$
\begin{aligned}
i_d = & I_{p1}\cos(\alpha_p+\theta_0)+I_{n1}\cos(4\pi f_1 t-\alpha_n+\theta_0) \\
& +\sum_{k=1}^{\infty}[I_{bpk}\cos(4ks\pi f_1 t+\beta_{bpk}+\theta_0)+I_{bnk}\cos(4ks\pi f_1 t-\beta_{bpk}-\theta_0)]
\end{aligned}
\tag{5.49}
$$

$$
\begin{aligned}
i_q = & -I_{p1}\sin(\alpha_p+\theta_0)+I_{n1}\sin(4\pi f_1 t-\alpha_n+\theta_0) \\
& -\sum_{k=1}^{\infty}[I_{bpk}\sin(4ks\pi f_1 t+\beta_{bpk}+\theta_0)+I_{bnk}\sin(4ks\pi f_1 t-\beta_{bpk}-\theta_0)]
\end{aligned}
\tag{5.50}
$$

From equations (5.49) and (5.50), it can be seen that the characteristic frequencies of different components of i_d and i_q change as follows: the positive sequence fundamental wave component changes into dc component, the negative sequence fundamental wave component changes into $2f_1$ component, and the characteristic frequency of rotor broken bar $(1+2ks)f_1$ changes into $2ksf_1$.

### 5.4.3.2　Composite fault simulation signal analysis

On the basis of the above principles, the asymmetric compound faults of stator and rotor were simulated and analyzed. During the simulation, fault resistors R_1 and R_2 were added to stator a-phase windings and rotor b-phase windings respectively. Figure 5.12(a)~(f) show the spectrum diagnosis results of the compound faults of stator and rotor to different degrees.

(a) rotor R_1=0.5Ω, stator R_2=0.5Ω　　　　　(b) rotor R_1=0.5Ω, stator R_2=1.5Ω
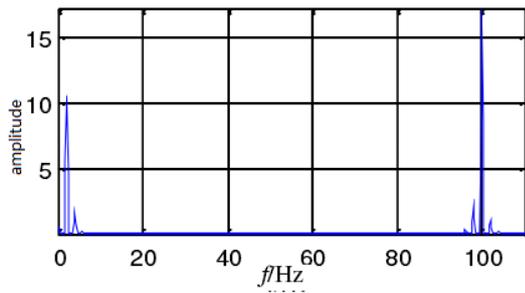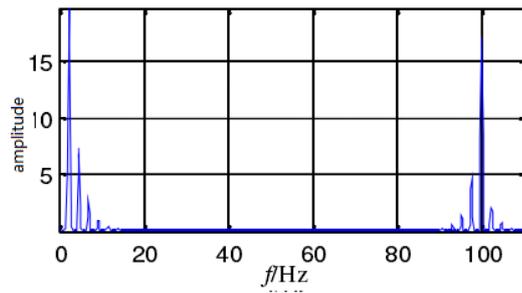
(c) rotor $R_1=1.0\Omega$, stator $R_2=0.5\Omega$ (d) rotor $R_1=1.0\Omega$, stator $R_2=1.5\Omega$
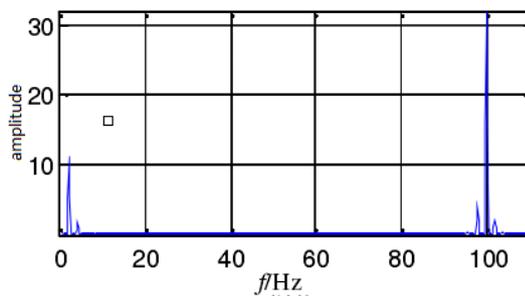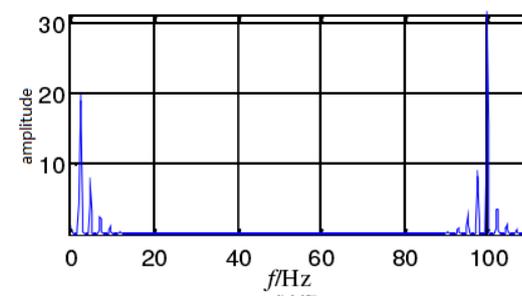
(e) rotor $R_1=1.0\Omega$, stator $R_2=0.5\Omega$ (f) rotor $R_1=1.0\Omega$, stator $R_2=1.5\Omega$
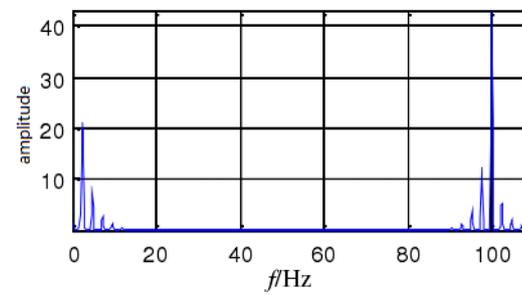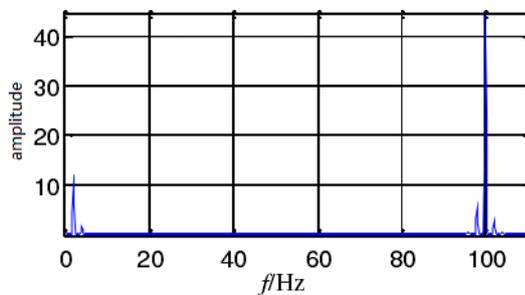

Figure 5.12 Stator and rotor complex fault spectrum diagram

As can be seen from the figure, the stator fault characteristic frequency is mainly reflected in the double frequency of power frequency component f_1 (i.e. 100Hz), and the rotor fault characteristic frequency is reflected in $2ksf_1$. When compound faults occur, the amplitude and quantity of power frequency and side frequency components are influenced by each other. It can be seen that the positive and negative sequence amplitudes of the fundamental wave

components of the stator current and the amplitude of the rotor broken bar components remain unchanged after the rotation coordinate transformation, (i.e. I_{p1}, I_{n1}, I_{bpk}, and I_{bnk}). According to relevant theories, the amplitude of the rotor's broken strip side frequency component is quite different from the power frequency component. In practical application, the rotor's fault side frequency feature is easily submerged in the double frequency feature. Therefore, it is necessary to separate rotor fault characteristic frequency from stator fault characteristic frequency so as to effectively realize the detection and diagnosis of stator fault and rotor fault.

Although state sensing and stator rotor fault diagnosis of ac motor have been completed to some extent through park vector transformation method, the current research on stator and rotor asymmetric faults remains at the qualitative diagnosis of fault state, which can further quantitatively determine the number of guide bars of rotor broken bars and stator short-circuit faults between turns.

6 Possible faults of rack & pinion and proposal method for fault diagnose

Heavy CNC machine tool working plane movement needs to be realized through rack and pinion. Rack and pinion transmission have the characteristics of high precision, large load and convenient maintenance. Although the manufacturing technology and performance reliability of the gear have been greatly improved, the structure of the gear transmission itself is relatively complex, the working environment is bad, plus human operation and other reasons, failure will inevitably occur.

For rack and pinion, the traditional maintenance methods mainly include after-service maintenance and regular maintenance. The failure of gearbox parts will aggravate the wear of other parts and expand the failure surface. Therefore, when the failure occurs, the maintenance will not only cause a shutdown, but also relatively high maintenance costs. In some important gearbox maintenance, the post-maintenance has been abandoned. Although regular maintenance has a certain planning, reducing the probability of sudden failure, but it cannot be avoided, and regular replacement will bring unnecessary waste. Adopting effective technical means and perfect monitoring system to monitor and diagnose the running state of gear can effectively avoid unnecessary losses caused by fault shutdown and regular maintenance. It has great research value and significance from both safety and economic aspects. [9]

6.1   Possible faults of rack and pinion

According to statistics, the proportion of gear fault types is: broken teeth account for 41%, tooth surface abnormality accounts for 31%, wear accounts for 10%, and other accounts for 18%.

Different types of faults are shown as follow:

Tooth surface wear: In the process of gnawing and gnawing, friction will occur on the upper and lower parts of the node. Under normal conditions, after a certain period of time, the tooth surface will become bright and smooth, and the tooth thickness will become thinner. If the gear manufacturing material is not good, the assembly tooth gap is too small, the lubrication condition is poor, the impact load is too large, will aggravate the wear, tooth surface will appear pull mark, concave and convex inequality, make the tooth profile change, tooth gap is larger, the degree of coincidence and stiffness decline, mesh vibration dynamic energy and noise will gradually increase.

Figure 6.1 tooth surface wear

Tooth surface abnormity: Including tooth pitting, peeling, gluing and abrasion. Meshing gear tooth moves in opposite direction under certain load, tooth surface will produce contact stress, when this stress exceeds the fatigue limit of material, will produce plastic deformation or crack, increase the friction coefficient of contact surface, make crack continues to extend, cause tooth surface metal small piece to flake off, form pitting to flake off. Gear under the condition of high speed and overloading, the local stress is larger, if the lubrication condition is bad, can make

the thinning of the lubricating oil film between gear teeth, increase friction, produce large amounts of heat can be collected at the same time, under the condition of high temperature and high pressure, relative motion tooth agglutinate phenomenon happens, the surface of the metal material was torn down, lead to irregular concave and convex surface.
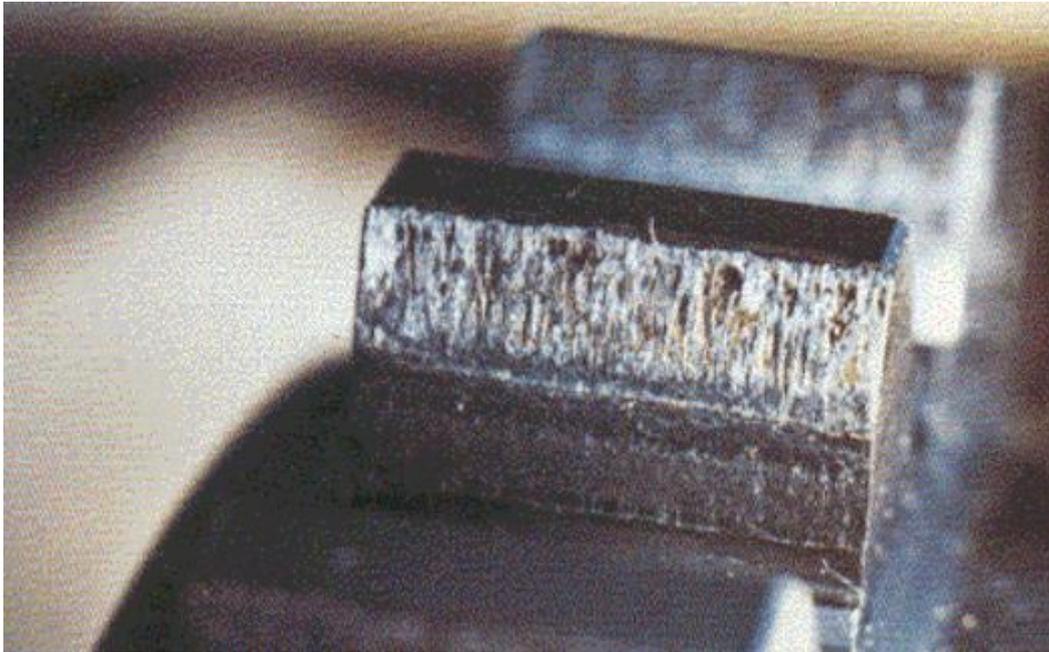
Figure 6.2 Tooth surface abnormity

Tooth broken: The meshing and rotating two teeth interact with each other on the contact surface of each other, and the contact surface will change due to the change of tooth gap or the instability of shaft. If the contact moves towards the top of a tooth, the bending stress borne by the tooth will increase, and the instantaneous impact overload may make the tooth break. Fatigue crack caused by normal repeated loading is one of the important causes of tooth fracture.

Figure 6.3 Tooth broken

6.2 The source of gear vibration

Gear transmission is to realize the transmission of power and motion state by multiple gear teeth at the end of the engagement of the former one and the latter one. Ideally, this process is stable, but due to tooth gap, elastic deformation, manufacturing and assembly errors and wear, pitting and peeling, broken teeth and other factors, the tooth meshing process will inevitably produce shock vibration phenomenon. Gear vibration is the reflection of dynamic response after dynamic excitation. Different causes will generate different excitation, which can be divided into normal meshing excitation and fault excitation. Analysis of the types and causes of excitation plays an important role in studying the meshing vibration mechanism of gears. The types and causes are as follows: [10]

(1) The internal motivation includes: stiffness motivation, error motivation and meshing impact motivation.

Stiffness motivation: The meshing stiffness of gears is small in the meshing of a pair of teeth, but large in the meshing of two pairs of teeth. It changes periodically repeatedly. No matter there is no error of the teeth, regular excitation force will be generated to make the gears subject

to dynamic excitation.

Error motivation: The tooth pitch error and tooth profile error generated after the processing, assembly and failure of gears make the meshing tooth profile of gears deviate from the ideal position, resulting in uneven force generated in the meshing region of different gears, resulting in unbalanced gear transmission and impact excitation.

Meshing impact motivation: There are tooth gaps between the teeth, and elastic deformation will also occur after loading, which will lead to changes in the meshing state between disengagement and contact when the teeth are biting or biting out. In this process, impact excitation will be generated.

(2) External motivation: The change of the external input load, the rotation imbalance of the shaft, coupling, bearing and other parts connected with the gear, will stimulate the gear meshing process.

6.3　　Vibration signal analysis

The acquisition of rack and pinion vibration signal needs to be realized by vibration detector. For the obtained vibration signal, the time domain to frequency domain conversion is required, the conversion method is not described here. The vibration detection method is explained by a case of vibration detection.
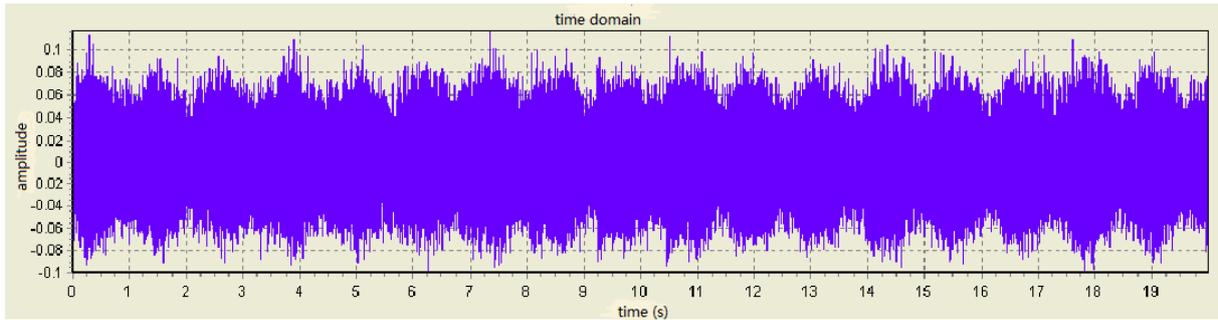
Figure 6.4 Normal working vibration waveform (time domain)
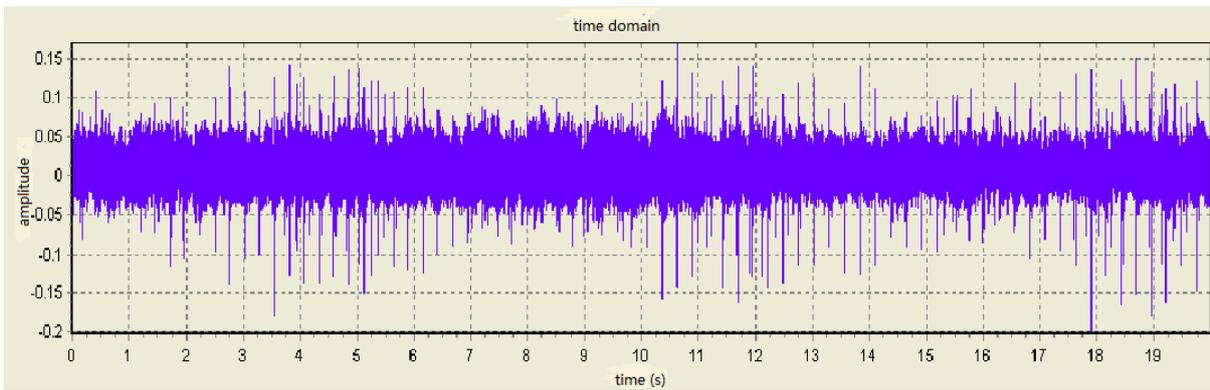
Figure 6.5 Abnormal working vibration waveform (time domain)

By comparing Figure 6.4 and Figure 6.5, significant shock is shown in Figure 6.5 which

means the gear system is working in abnormal condition.
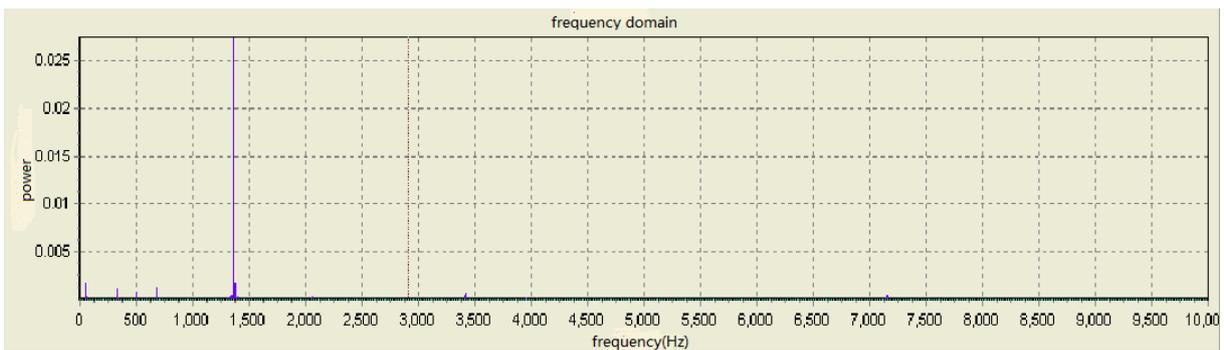
Figure 6.6 Normal working vibration waveform (frequency domain)
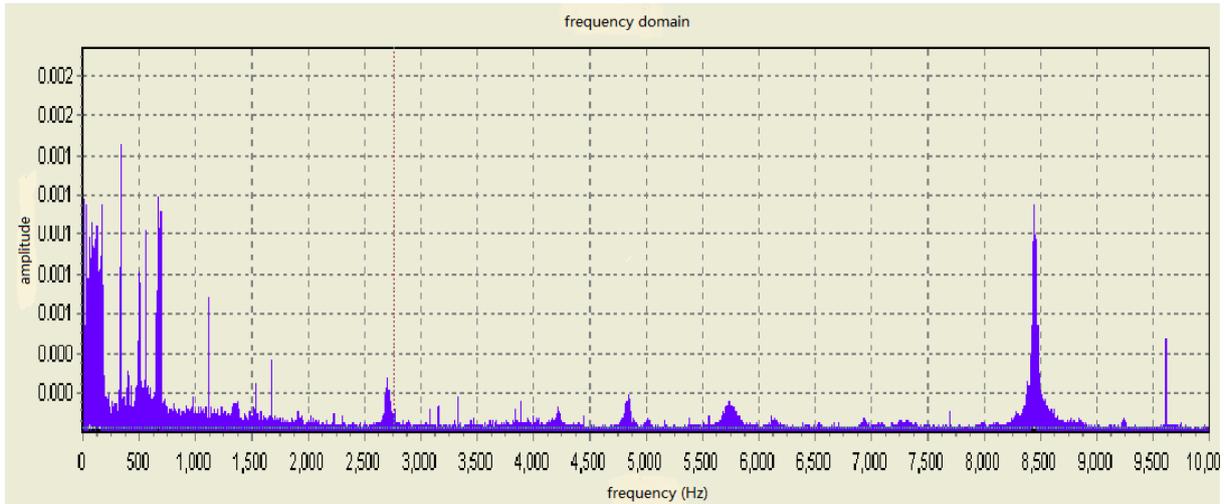
Figure 6.7 Abnormal working vibration waveform (frequency domain)

By comparing Figure 6.6 and Figure 6.7, significant peaks appear in both low frequency field and high frequency field which means that gear system is working in abnormal condition.

7 Conclusion and development prospect

This paper describes tandem motor and rack pinion system which is an anti-backlash method used in working table movement for heavy CNC machine. Then it describes possible faults of tandem motors which can be caused by both mechanical reasons and electrical reasons. Both of the two types of reasons may lead to system subnormal working even damage the whole system. In chapter 3, three types of maintenance methods are introduced and the predictive maintenance method should be used in tandem motor and rack pinion system due to its significant advantages.

Under the trend of industry 4.0, the working conditions of almost all working elements need to be monitored, and the tandem motor and rack pinion system is no exception. Monitoring equipment and signal analysis provides powerful guarantee for predictive maintenance management.

In chapter 4, 10 types of possible methods to detect errors of tandem motors are introduced. Every single method has both advantages and disadvantages considering the detecting performance and the cost. MCSA is deeply described in this paper due to its nice performance, economic cost and less additional equipment. The reason why motor monitoring occupies a larger space than rack pinion monitoring is that errors even damage are easier to happen on tandem motor than rack pinion.

During predictive maintenance management process, measures should be taken by manager as soon as the error which has an impact on production process appears. If a minor problem of is detected during production, the manager may choose to keep the machine working, but manager should arrange maintenance or repair work as soon as possible during the spare time of the

CNC machine, this can achieve small effect even no effect on production efficiency and at the same reduce the cost of repairing.

This paper just introduces some basic monitoring methods and signal analysis methods, but doesn't involve advanced and complex ones. MCSA is an excellent method but at present, the research of stator rotor asymmetry is still limited to qualitative diagnosis, and the number of guide bars of rotor broken bars and stator short-circuit between turns can be further quantitatively determined. With the development of expert system, fuzzy control, neural network, genetic algorithm and other artificial intelligence methods, the rapidity and accuracy of condition diagnosis will be further improved.

8 Reference

[1] Yuan Miao. Dual-motor servo systems with backlash for Heavy machine rotary table. Huazhong University of Science and Technology Wuhan, Hubei 430074, P. R. China; May, 2015.

[2] Applications Engineer Wittenstein Inc. Bartlett, Ill. Comparing Performance and Efficiency of Linear Motors, Ball Screws, and Rack-and-Pinion Drives. Feb 03, 2010.

[3] R. Keith Mobley. Maintenance fundamentals. 2004

[4] Olav Vaag Thorsen, Senior Member, IEEE, and Magnus Dalva, Member, IEEE. Failure Identification and Analysis for High-Voltage Induction Motors in the Petrochemical Industry. IEEE transactions on industry applications, vol.35, No.4, July/August 1999.

[5] Paulo Antonio Delgado-Arredondo, Daniel Morinigo-Sotelo, Roque Alfredo Osornio-Rios, Juan Gabriel Avina-Cervantes, Horacio Rostro-Gonzalez, Rene de Jesus Romero-Troncoso. Methodology for fault detection in induction motors via sound and vibration signals. Received 22 January 2016, received in revised form 7 May 2016, Accepted 20 June 2016, Available online 1 July 2016.

[6] David Lopez-P´erez and Jose Antonino-Daviu. Application of Infrared Thermography to Failure Detection in Industrial Induction Motors: Case Stories. IEEE transactions on industry applications, vol.53, No.3, May/June 2017.

[7] William T. Thomson and Mark Fenger. current signature analysis to detect induction motor faults. IEEE Industry Applications Magazine, July/August 2001.

[8] Li Junyao. Current Signature Analysis and Health Sensing System Implementation for AC

Motor. Graduate School of National University of Defense Technology November, 2013

[9] Sanjay Kumara, Deepam Goyalb, Rajeev K. Dangc, Sukhdeep S. Dhamib, B.S. Pablab. Condition based maintenance of bearings and gears for fault detection – A review. 2017 Elsevier Ltd.

[10] Lai Dabo. Study on feature extraction and analysis technology for a gearbox fault vibration signal. University of Electronic Science and Technology of China, June 2013.